MKPH-T-99-7.

Complete Sets of Polarization Observables in Electromagnetic Deuteron Break-up * †

Hartmuth Arenhövel[1], Winfried Leidemann[2], and Edward L. Tomusiak[3]
[1]Institut für Kernphysik, Johannes Gutenberg-Universität,
D-55099 Mainz, Germany
[2]Dipartimento di Fisica, Università di Trento, and
Istituto Nazionale di Fisica Nucleare, Gruppo collegato di Trento,
I-38050 Povo, Italy
[3]Department of Physics and Engineering Physics
and Saskatchewan Accelerator Laboratory,
University of Saskatchewan, Saskatoon, Canada S7N 0W0

arXiv:nucl-th/9905029v1 14 May 1999

For deuteron photo- and electrodisintegration the selection of complete sets of polarization observables is discussed in detail by applying a recently developed new criterion for the check of completeness of a chosen set of observables. The question of ambiguities and their resolution by considering additional observables is discussed for a numerical example, for which the role of experimental uncertainties is also investigated. Furthermore, by inversion of the expressions of the observables as hermitean forms in the t-matrix elements a bilinear term of the form $t_{j'}^* t_j$ can be given as a complex linear form in the observables from which an explicit solution for t_j in terms of observables can be obtained. These can also be used to select sets of observables for the explicit representation of the t-matrix.

I. INTRODUCTION

Complete information on the dynamics of a reaction is contained in its reaction or t-matrix. Thus its determination is most desirable in order to provide a basis for a detailed comparison with any theoretical model. In general, the reaction matrix elements are complex numbers for which one phase remains undetermined, i.e. arbitrary. This means, if ones has n independent t-matrix elements, one needs at least $2n-1$ independent observables for a complete determination of all matrix elements, although in general some discrete ambiguities remain with such a minimal number of observables. On the other hand, since the number of linearly independent observables is n^2, the question arises of how one can decide whether a given set of $2n-1$ polarization observables of a reaction constitutes a complete set from which the reaction matrix can be reconstructed. In a recent paper [1] we have derived a general criterion which allows one to decide this question unambiguously. In that work we also have illustrated this criterion by applying it to the longitudinal observables of deuteron electrodisintegration.

In the present work, we have extended this analysis to all polarization observables of electromagnetic deuteron break-up, i.e., photo- and electrodisintegration. To this end we briefly review in Sect. II our previous work on the general formalism of polarization observables [2–4], for which we had chosen a particular basis for the representation of the t-matrix elements, and generalize it to arbitrary orientations of the initial and final spin quantization axes. Sect. III is devoted to the application of our new criterion to the transverse polarization observables, deriving explicitly groups of possible complete sets. We will also discuss for a specific numerical example the discrete ambiguities which can appear for a complete set with a minimal number of observables. Furthermore, we will analyze in this section the influence of possible experimental errors in such an analysis and derive bounds, which specific polarization observables have to fulfil. In Sect. IV we will show that an analytic solution of the reaction matrix elements in terms of structure functions is possible. This is achieved by inverting the formal expressions of the structure functions as hermitean forms in the reaction matrix elements yielding the bilinear terms $t_{j'}^* t_j$ as linear superpositions of structure functions. Their explicit form depends on the chosen basis for the initial and final hadronic spin states. Several choices will be discussed in detail. We will close with a summary and outlook. Specific details and complimentary material are presented in several appendices. In particular, in Appendix A a detailed comparison between our formalism and the one of Dmitrasinovic and Gross [6] is given.

---

*Dedicated to Professor Walter Glöckle on the occasion of his 60th birthday

†Supported by the Deutsche Forschungsgemeinschaft (SFB 443) and the National Science and Engineering Research Council of Canada

II. GENERAL FORMALISM

In this section we will briefly review the general formalism of polarization observables in deuteron photo- and electrodisintegration - the latter in the one-photon-approximation - as presented in detail in [3,4] with some generalization to arbitrary quantization axes for the initial and final hadronic states.

We start from Eq. (58) of [4] for a general observable X in exclusive deuteron electrodisintegration

$$\begin{aligned}
\mathcal{O}(X) &= P(X)S_0 \\
&= c(k_1^{lab}, k_2^{lab}) \sum_{I=0}^{2} P_I^d \sum_{M=0}^{I} \Big\{ (\rho_L f_L^{IM}(X) + \rho_T f_T^{IM}(X) + \rho_{LT} f_{LT}^{IM+}(X) \cos\phi \\
&\qquad + \rho_{TT} f_{TT}^{IM+}(X) \cos 2\phi) \cos(M\tilde{\phi} - \bar{\delta}_I^X \frac{\pi}{2}) \\
&\quad - (\rho_{LT} f_{LT}^{IM-}(X) \sin\phi + \rho_{TT} f_{TT}^{IM-}(X) \sin 2\phi) \sin(M\tilde{\phi} - \bar{\delta}_I^X \frac{\pi}{2}) \\
&\quad + h \Big[(\rho'_T f'^{IM}_T(X) + \rho'_{LT} f'^{IM-}_{LT}(X) \cos\phi) \sin(M\tilde{\phi} - \bar{\delta}_I^X \frac{\pi}{2}) \\
&\qquad + \rho'_{LT} f'^{IM+}_{LT}(X) \sin\phi \cos(M\tilde{\phi} - \bar{\delta}_I^X \frac{\pi}{2}) \Big] \Big\} d^I_{M0}(\theta_d) \,, \qquad (1)
\end{aligned}$$

where S_0 denotes the unpolarized differential cross section and

$$c(k_1^{lab}, k_2^{lab}) = \frac{\alpha}{6\pi^2} \frac{k_2^{lab}}{k_1^{lab} q_\nu^4} \,. \qquad (2)$$

Here α is the fine structure constant and k_1^{lab} and k_2^{lab} denote the lab frame momenta of the initial and the scattered electrons, respectively, while $q_\nu^2 = q_0^2 - \vec{q}^{\,2}$ is the squared four momentum transfer ($q = k_1 - k_2$). The virtual photon density matrix is given by

$$\rho_L = -\beta^2 q_\nu^2 \frac{\xi^2}{2\eta} \,, \qquad \rho_{LT} = -\beta q_\nu^2 \frac{\xi}{\eta} \sqrt{\frac{\xi+\eta}{8}} \,, \qquad (3)$$

$$\rho_T = -\frac{1}{2} q_\nu^2 (1 + \frac{\xi}{2\eta}) \,, \qquad \rho_{TT} = q_\nu^2 \frac{\xi}{4\eta} \,, \qquad (4)$$

$$\rho'_T = -\frac{1}{2} q_\nu^2 \sqrt{\frac{\xi+\eta}{\eta}} \,, \qquad \rho'_{LT} = -\frac{1}{2} \beta q_\nu^2 \frac{\xi}{\sqrt{2\eta}} \,, \qquad (5)$$

with

$$\beta = \frac{|\vec{q}^{\,lab}|}{|\vec{q}^{\,c}|}, \quad \xi = -\frac{q_\nu^2}{(\vec{q}^{\,lab})^{\,2}}, \quad \eta = \tan^2(\frac{\theta_e^{lab}}{2}) \,, \qquad (6)$$

where θ_e^{lab} denotes the electron scattering angle in the lab system and β expresses the boost from the lab system to the frame in which the hadronic tensor is evaluated and $\vec{q}^{\,c}$ denotes the momentum transfer in this frame. For real photons only the transverse structure functions contribute and one has to replace in (1) $c(k_1^{lab}, k_2^{lab}) \to 1/3$ and the virtual photon density matrix by

$$\begin{array}{lll} \rho_L \to 0, & \rho_{LT} \to 0, & \rho'_{LT} \to 0, \\ \rho_T \to \frac{1}{2}, & h\rho'_T \to \frac{1}{2} P_c^\gamma, & \rho_{TT} \to -\frac{1}{2} P_l^\gamma \,, \end{array} \qquad (7)$$

where P_l^γ and P_c^γ denote the degree of linear and circular photon polarization, respectively.

Often the hadronic tensor and thus the observables are calculated in the final np c.m. system. This system, which sometimes is also called anti-lab system, moves in the laboratory with total momentum $\vec{q}^{\,lab}$. In the following we will adopt this system, i.e. $\vec{q}^{\,c} = \vec{q}^{\,c.m.}$. The initial state is characterized by the photon helicity λ ($= \pm 1$ for real and $= 0, \pm 1$ for virtual photons), and the deuteron spin projection λ_d with respect to a chosen quantization axis. Correspondingly, the final np system is characterized by the relative np momentum $\vec{p}_{np}$ and the spin quantum numbers of the two nucleons, either in the uncoupled representation (λ_p, λ_n) or the coupled one (s, m_s) with respect to some quantization axis. The deuteron polarization is described by spherical orientation tensors $\tau_M^{[I]}$ with $I = 0, 1, 2$, and for the outgoing nucleon polarization components including no polarization one has 16 independent operators acting in

the final two-nucleon spin space according to all combinations of the four operators $(1,\,\vec{\sigma})$ of each of the two nucleons. The components of the spin operators of both particles refer to the reference frame associated with the final np c.m. system denoted by $(x,\,y,\,z)$ where the z-axis is parallel to $\vec{p}_{np}$ in the reaction plane and its y-axis parallel to $\vec{q}\times\vec{p}_{np}$, i.e. perpendicular to the reaction plane. Thus the polarization components of particle "1" (here the proton) are chosen according to the Madison convention while for particle "2" (neutron) the y- and z-components of $\vec{P}$ have to be reversed in order to comply with this convention. The spherical angles of proton and neutron momenta with respect to the reference frame associated with the reaction plane in the c.m. system are $\theta_p^{c.m.}=\theta$, $\phi_p^{c.m.}=\phi$ and $\theta_n^{c.m.}=\pi-\theta$, $\phi_n^{c.m.}=\phi+\pi$ (see Fig. 1).

The basic quantities which determine the differential cross section and the outgoing nucleon polarization components for beam and target polarization and which contain the complete information on the dynamical properties of the NN system available in deuteron photo- and electrodisintegration are the structure functions $f_\alpha^{(\prime)IM}(X)$, where $\alpha\in\{L,T,LT,TT\}$ characterizes the diagonal and interference contributions from the longitudinal and transverse polarizations of the virtual or real photon, and (I,M) the deuteron polarization tensors. The polarization components of the outgoing two nucleons are represented by $X=(x_{\alpha'}x_\alpha)$ where the first entry refers to the proton and the second to the neutron. Explicitly we use $x_1=x$, $x_2=y$, $x_3=z$, whereas $x_0=1$ describes the case of no polarization. Furthermore, for the explicit notation of a polarization component of only one nucleon we use an index 1 or 2 in case of proton or neutron, respectively, i.e., instead of e.g. $X=(x1)$ we use $X=x_1$ or instead of $X=(1z)$ we use $X=z_2$. An explicit listing is given in Table I where we also have indicated the division of the observables into two sets, named A and B, according to their behaviour under a parity transformation as discussed in [3]. Formal expressions of structure functions have also been derived in [6] with respect to the socalled hybrid basis. The relation of these structure functions to ours is established in Appendix A.

In [4] we have expressed all structure functions in terms of real or imaginary parts of the quantities $\mathcal{U}_X^{\lambda'\lambda IM}$

$$f_L^{IM}(X)=\frac{2}{1+\delta_{M0}}\Re e\left(i^{\bar\delta_I^X}\mathcal{U}_X^{00IM}\right)\,, \tag{8}$$

$$f_T^{IM}(X)=\frac{4}{1+\delta_{M0}}\Re e\left(i^{\bar\delta_I^X}\mathcal{U}_X^{11IM}\right)\,, \tag{9}$$

$$f_{LT}^{IM\pm}(X)=\frac{4}{1+\delta_{M0}}\Re e\left[i^{\bar\delta_I^X}\left(\mathcal{U}_X^{01IM}\pm(-)^{I+M+\delta_{X,\,B}}\mathcal{U}_X^{01I-M}\right)\right]\,, \tag{10}$$

$$f_{TT}^{IM\pm}(X)=\frac{2}{1+\delta_{M0}}\Re e\left[i^{\bar\delta_I^X}\left(\mathcal{U}_X^{-11IM}\pm(-)^{I+M+\delta_{X,\,B}}\mathcal{U}_X^{-11I-M}\right)\right]\,, \tag{11}$$

$$f_T^{\prime IM}(X)=\frac{4}{1+\delta_{M0}}\Re e\left(i^{1+\bar\delta_I^X}\mathcal{U}_X^{11IM}\right)\,, \tag{12}$$

$$f_{LT}^{\prime IM\pm}(X)=\frac{4}{1+\delta_{M0}}\Re e\left[i^{1+\bar\delta_I^X}\left(\mathcal{U}_X^{01IM}\pm(-)^{I+M+\delta_{X,\,B}}\mathcal{U}_X^{01I-M}\right)\right]\,. \tag{13}$$

Here we have introduced

$$\bar\delta_I^X:=(\delta_{X,B}-\delta_{I1})^2\,,\ \text{and}\ \delta_{X,B}:=\begin{cases}1 & \text{for } X\in B\\ 0 & \text{for } X\in A\end{cases}\,, \tag{14}$$

distinguishing the two sets of observables A and B.

The total number of structure functions listed in (8) through (13) is $2n^2$ [4], where the number n of independent matrix elements is 12 in photo- and 18 in electrodisintegration. This is twice as much as the number of linearly independent observables. Indeed, one finds n^2 linear relations among the structure functions (see [3] for photo- and [4] for electrodisintegration), reducing the total number of linearly independent observables to the required n^2. On the other hand, since each reaction matrix element is in general a complex number, but one overall phase is undetermined, a set of $2n-1$ properly chosen observables should suffice to determine completely all matrix elements. This seeming contradiction is resolved by the observation, that the linearly independent observables are not completely independent of each other in a more general sense. In fact, since any bilinear form $t_{j'}^*t_j$ can be given as a linear expression in the observables (see Sect. IV), one can find exactly $(n-1)^2$ quadratic relations between them as is shown in Appendix B, reducing the total number of independent observables just to the required number. Consequently, one can determine all matrix elements from $2n-1$ properly chosen observables. However, one should keep in mind that the solution is in general not unique but contains discrete ambiguities.

Now we will proceed to review the explicit representation of the structure functions as quadratic hermitean forms in the t-matrix elements. In the foregoing expressions, the $\mathcal{U}$'s are given as bilinear forms in the reaction matrix elements, i.e., for $X=(x_{\alpha'}x_\alpha)$

$$\mathcal{U}^{\lambda'\lambda IM}_{\alpha'\alpha} = \sum_{m'_1 m'_2 \lambda'_d m_1 m_2 \lambda_d} t^*_{m'_1 m'_2 \lambda' \lambda'_d} \langle m'_1 m'_2 | \Omega_{\alpha'}(1) \Omega_\alpha(2) | m_1 m_2 \rangle t_{m_1 m_2 \lambda \lambda_d} \langle \lambda_d | \tau^{[I]}_M | \lambda'_d \rangle \,, \tag{15}$$

where (m_1, m_2) stands for the spin quantum numbers of the outgoing nucleons, either in the coupled representation (s, m_s) or in the uncoupled one (λ_p, λ_n), and the spin operators for the outgoing nucleons are denoted by

$$\Omega_\alpha(i) = \sigma_\alpha(i) \,, \quad (i = 1, 2), \tag{16}$$

with $\alpha = 0, \ldots, 3$ and $\sigma_0 = \mathbb{1}_2$. In view of the angular momentum algebra it is useful to switch to a spherical representation replacing the cartesian components of the spin operators by their spherical ones

$$\Omega_\alpha(i) = \sum_{\tau=0,1} \sum_{\nu=-\tau}^{\tau} s^{\tau\nu}_\alpha \, \Omega_{\tau\nu}(i) \,, \tag{17}$$

$$\Omega_{\tau\nu}(i) = \sigma^{[\tau]}_\nu(i) \qquad (\tau = 0,\, 1), \tag{18}$$

defining $\sigma^{[0]} = \mathbb{1}_2$ and $\sigma^{[1]}_\nu = \sigma_\nu$. The transformation matrix is defined by

$$s^{\tau\nu}_\alpha = \bar{c}(\alpha) \, \delta_{\tau \widetilde{\tau}(\alpha)} \, (\delta_{\nu \widetilde{\nu}(\alpha)} + \hat{c}(\alpha) \, \delta_{\nu - \widetilde{\nu}(\alpha)}) \,, \tag{19}$$

with

$$\begin{aligned} &\hat{c}(\alpha) = \delta_{\alpha 2} - \delta_{\alpha 1} \,, \;\; \bar{c}(\alpha) = \begin{cases} 1 & \text{for } \alpha = 0,\, 3 \\ \frac{i^{-\alpha-1}}{\sqrt{2}} & \text{for } \alpha = 1,\, 2 \end{cases} \,, \\ &\widetilde{\tau}(\alpha) = 1 - \delta_{\alpha 0} \,, \quad \widetilde{\nu}(\alpha) = \begin{cases} 0 & \text{for } \alpha = 0,\, 3 \\ 1 & \text{for } \alpha = 1,\, 2 \end{cases} \,. \end{aligned} \tag{20}$$

Explicit expressions are listed in Table II. For later purposes we note the inverse transformation from spherical to cartesian components

$$\Omega_{\tau\nu}(i) = \sum_{\alpha=0}^{3} c^\alpha_{\tau\nu} \, \Omega_\alpha(i) \,, \tag{21}$$

where we have defined

$$c^\alpha_{\tau\nu} = c(\nu)(\delta_{\alpha a(\tau,\nu)} + i\nu \, \delta_{\alpha b(\tau,\nu)}) \,, \tag{22}$$

with

$$c\,(\nu) = -\frac{\nu}{\sqrt{2}} \, \delta_{|\nu|1} + \delta_{\nu 0} \,, \quad a\,(\tau, \nu) = 3\tau - 2|\nu| \,, \quad b\,(\tau, \nu) = 3\tau - |\nu| \,. \tag{23}$$

Then the transformation of the $\mathcal{U}$'s to spherical components is given by

$$\mathcal{U}^{\lambda'\lambda IM}_{\alpha'\alpha} = \sum_{\tau'\nu'\tau\nu} s^{\tau'\nu'}_{\alpha'} \, s^{\tau\nu}_\alpha \, \mathcal{U}^{\lambda'\lambda IM}_{\tau'\nu'\tau\nu} \tag{24}$$

where $\mathcal{U}^{\lambda'\lambda IM}_{\tau'\nu'\tau\nu}$ is defined as in (15) with $\Omega_\alpha(i)$ being replaced by the spherical components of (18).

The explicit form in terms of the t-matrix elements depends on the representation for the initial and final spin states. As mentioned above, we will consider two cases, an uncoupled representation with spin quantum numbers $(\lambda_p,\, \lambda_n)$ and a coupled one with $(s,\, m_s)$. The canonical direction of the quantization axis for the initial deuteron state is the incoming photon momentum and for the final state the direction of the relative np momentum in the final state c.m. frame. In the uncoupled representation this is called the helicity representation and for the coupled case we have named it the standard representation. The representations obey the following symmetry relation if parity is conserved

$$t_{-\lambda_p - \lambda_n - \lambda - \lambda_d} = (-)^{\lambda_p + \lambda_n + \lambda + \lambda_d} \, t_{\lambda_p \lambda_n \lambda \lambda_d} \,, \tag{25}$$

$$t_{s - m_s - \lambda - \lambda_d} = (-)^{1 + s + m_s + \lambda + \lambda_d} \, t_{s m_s \lambda \lambda_d} \,. \tag{26}$$

The transformation from one representation to the other is simply given by a Clebsch-Gordan coefficient

$$t_{\lambda_p\lambda_n\lambda\lambda_d} = \sum_{sm_s}(-)^{m_s}\hat{s}\begin{pmatrix}\frac{1}{2} & \frac{1}{2} & s\\ \lambda_p & \lambda_n & -m_s\end{pmatrix} t_{sm_s\lambda\lambda_d}\,. \tag{27}$$

A third representation called hybrid basis, where the quantization axis is chosen perpendicular to the reaction plane, was introduced in [6]. We shall also consider this basis later on.

For later purposes, however, it is useful to allow for arbitrary directions of the quantization axis. Thus we will consider general rotations $R_d(\alpha_d,\beta_d,\gamma_d)$ of the initial deuteron state and $R_f(\alpha_f,\beta_f,\gamma_f)$ of the final two-nucleon state. Denoting a rotated state by a subscript "R", i.e. $|jm\rangle_R$, one has

$$\langle jm|j\bar{m}\rangle_R = D^j_{m\bar{m}}(R)\,, \tag{28}$$

where the D-matrices are taken in the convention of [5]. Correspondingly, the initial and final state irreducible spin operators transform under a rotation R as

$$R^{-1}O^{[j]}_m R = \sum_{m'} O^{[j]}_{m'} D^j_{m'm}(R^{-1})\,. \tag{29}$$

Then the reaction matrix elements are transformed according to

$$\begin{aligned} t^{R_fR_d}_{\bar{\lambda}_p\bar{\lambda}_n\lambda\bar{\lambda}_d} &= \sum_{\lambda_p\lambda_n\lambda_d} {}_{R_f}\langle\tfrac{1}{2}\bar{\lambda}_p|\tfrac{1}{2}\lambda_p\rangle\,{}_{R_f}\langle\tfrac{1}{2}\bar{\lambda}_n|\tfrac{1}{2}\lambda_n\rangle\, t_{\lambda_p\lambda_n\lambda\lambda_d}\,\langle 1\lambda_d|1\bar{\lambda}_d\rangle_{R_d} \\ &= \sum_{\lambda_p\lambda_n\lambda_d} D^{\frac{1}{2}}_{\bar{\lambda}_p\lambda_p}(R_f^{-1})\, D^{\frac{1}{2}}_{\bar{\lambda}_n\lambda_n}(R_f^{-1})\; t_{\lambda_p\lambda_n\lambda\lambda_d}\, D^1_{\lambda_d\bar{\lambda}_d}(R_d) \end{aligned} \tag{30}$$

for the uncoupled representation, and

$$t^{R_fR_d}_{s\bar{m}_s\lambda\bar{\lambda}_d} = \sum_{m_s\lambda_d} D^s_{\bar{m}_sm_s}(R_f^{-1})\, t_{sm_s\lambda\lambda_d}\, D^1_{\lambda_d\bar{\lambda}_d}(R_d) \tag{31}$$

for the coupled one. The symmetry of (25) and (26) translates into a somewhat more involved relation for the case of arbitrary rotations R_f and R_d, namely one finds

$$t^{R_fR_d}_{-\lambda_p-\lambda_n-\lambda-\lambda_d} = (-)^{\lambda_p+\lambda_n+\lambda+\lambda_d}\, t^{\bar{R}_f\bar{R}_d}_{\lambda_p\lambda_n\lambda\lambda_d}\,, \tag{32}$$

$$t^{R_fR_d}_{s-m_s-\lambda-\lambda_d} = (-)^{1+s+m_s+\lambda+\lambda_d}\, t^{\bar{R}_f\bar{R}_d}_{sm_s\lambda\lambda_d}\,, \tag{33}$$

where we have defined for a rotation $R=(\alpha,\beta,\gamma)$ an associated rotation by $\bar{R}=(-\alpha,\beta,-\gamma)$. We note in passing that the transformation to the hybrid basis of [6] is achieved by a simultaneous rotation around the x-axis by $\pi/2$, i.e., $R_f=R_d$ with $(\alpha,\beta,\gamma)=(\pi/2,\pi/2,-\pi/2)$.

For the $\mathcal{U}$'s, the evaluation of the spin operators in (15) leads to

$$\mathcal{U}^{\lambda'\lambda IM}_{\tau'\nu'\tau\nu} = \sum_{m_1'm_2'\lambda_d'm_1m_2\lambda_d} C^{m_1'm_2'\lambda_d'}_{m_1m_2\lambda_d}(\tau'\nu'\tau\nu IM)\,(t^{R_fR_d}_{m_1'm_2'\lambda'\lambda_d'})^*\, t^{R_fR_d}_{m_1m_2\lambda\lambda_d}\,, \tag{34}$$

where one has for the uncoupled representation

$$C^{\lambda_p'\lambda_n'\lambda_d'}_{\lambda_p\lambda_n\lambda_d}(\tau'\nu'\tau\nu IM) = 2\sqrt{3}\,\Omega^{\tau'\nu'}_{\frac{1}{2}\lambda_p'\frac{1}{2}\lambda_p}(R_f^{-1})\,\Omega^{\tau\nu}_{\frac{1}{2}\lambda_n'\frac{1}{2}\lambda_n}(R_f^{-1})\,\Omega^{IM}_{1\lambda_d1\lambda_d'}(R_d^{-1})\,. \tag{35}$$

Here we have introduced the quantities

$$\Omega^{JM}_{j'm'jm}(R) = (-)^{j'-m'}\hat{J}\sum_{M'}\begin{pmatrix} j' & J & j\\ -m' & M' & m\end{pmatrix} D^J_{M'M}(R)\,, \tag{36}$$

for which we would like to note the following properties:
(i) symmetry

$$\Omega^{JM}_{jmj'm'}(R) = (-)^{J+m-m'}\Omega^{JM}_{j'-m'j-m}(R)\,, \tag{37}$$

$$(\Omega^{JM}_{j'm'jm}(R))^* = (-)^{j+m+j'+m'+J+M}\Omega^{J-M}_{j'-m'j-m}(R)\,, \tag{38}$$

(ii) orthogonality

$$\sum_{JM}(\Omega^{JM}_{j'm'jm}(R))^*\,\Omega^{JM}_{j'\bar{m}'j\bar{m}}(R) = \delta_{\bar{m}'m'}\delta_{\bar{m}m}\,. \tag{39}$$

Correspondingly, one finds for the coupled representation

$$C^{s'm'_s\lambda'_d}_{sm_s\lambda_d}(\tau'\nu'\tau\nu IM) = (-)^{\tau'+\tau}2\sqrt{3}\,\hat{\tau}'\hat{\tau}\hat{s}'\hat{s}\,\Omega^{IM}_{1\lambda_d1\lambda'_d}(R_d^{-1}) \sum_{S\sigma}(-)^{\sigma}\hat{S}\begin{pmatrix}\tau' & \tau & S\\ \nu' & \nu & -\sigma\end{pmatrix}\begin{Bmatrix}\frac{1}{2} & \frac{1}{2} & \tau'\\ \frac{1}{2} & \frac{1}{2} & \tau\\ s' & s & S\end{Bmatrix}\Omega^{S\sigma}_{s'm'_ssm_s}(R_f^{-1})\,. \tag{40}$$

For both cases one easily finds with the help of (39) and the orthogonality properties of the $3j$- and $9j$-symbols the orthogonality relation

$$\sum_{\tau'\nu'\tau\nu IM}(C^{\bar{m}'_1\bar{m}'_2\bar{\lambda}'_d}_{\bar{m}_1\bar{m}_2\bar{\lambda}_d}(\tau'\nu'\tau\nu IM))^*\,C^{m'_1m'_2\lambda'_d}_{m_1m_2\lambda_d}(\tau'\nu'\tau\nu IM) = 12\delta_{\bar{m}'_1m'_1}\delta_{\bar{m}'_2m'_2}\delta_{\bar{\lambda}'_d\lambda'_d}\delta_{\bar{m}_1m_1}\delta_{\bar{m}_2m_2}\delta_{\bar{\lambda}_d\lambda_d}\,, \tag{41}$$

where one has $(m_1,\,m_2) = (\lambda_p,\,\lambda_n)$ for the uncoupled case, and $(m_1,\,m_2) = (s,\,m_s)$ for the coupled case. It is worth mentioning, that the $\mathcal{U}$'s do not depend on the choice of representation as is apparent from the general definition in (15) as a trace with respect to the spin quantum numbers, because it is invariant under unitary transformations of the spin states.

The $\mathcal{U}$'s possess the following symmetry properties

$$\left(\mathcal{U}^{\lambda'\lambda IM}_X\right)^* = (-)^M\mathcal{U}^{\lambda\lambda' I-M}_X = (-)^{\lambda'+\lambda+I+\delta_{X,B}}\mathcal{U}^{-\lambda-\lambda' IM}_{\overline{X}}\,, \tag{42}$$

or for the spherical representation

$$\left(\mathcal{U}^{\lambda'\lambda IM}_{\tau'\nu'\tau\nu}\right)^* = (-)^{M+\nu'+\nu}\mathcal{U}^{\lambda\lambda' I-M}_{\tau'-\nu'\tau-\nu} = (-)^{\lambda'+\lambda+I+\tau'+\tau}\mathcal{U}^{-\lambda-\lambda' IM}_{\tau'\nu'\tau\nu}\,. \tag{43}$$

These relations can be proven most easily using (25) or (26) in conjunction with (37)-(38) for $R_f = R_d = (0,0,0)$, i.e., for the helicity or standard representation.

III. GENERAL CRITERION FOR COMPLETE SETS OF OBSERVABLES

We will now address the question whether a set of $2n-1$ observables, chosen from the set of n^2 linearly independent observables, constitutes a complete set. In [1] we have derived a general criterion which allows one to decide this question uniquely. Before applying it to the present reaction, we will give first a brief outline of the main result of [1].

Any observable in a reaction with n independent matrix elements can be represented by an $n\times n$ hermitean form f^α in the complex n-dimensional variable z

$$f^\alpha(z) = \frac{1}{2}\sum_{j'j}z^*_{j'}F^\alpha_{j'j}z_j\,, \tag{44}$$

where hermiticity requires

$$(F^\alpha_{j'j})^* = F^\alpha_{jj'}\,, \tag{45}$$

and z comprises all independent reaction matrix elements labeled by j.

For the application of our criterion one first has to rewrite the hermitean form in (44) into a real quadratic form by introducing

$$z = x + iy\,, \tag{46}$$

$$F^\alpha = A^\alpha + i\,B^\alpha\,, \tag{47}$$

where A^α and B^α are real matrices, and A^α is symmetric whereas B^α is antisymmetric. Considering further the fact that one overall phase is arbitrary, one may choose $y_{j_0} = 0$ for one index j_0 and then one finds for the given observable

$$f^\alpha(x+iy) = \frac{1}{2}\Big[\sum_{j'j} x_{j'} A^\alpha_{j'j} x_j + \sum_{\tilde{j}'\tilde{j}} y_{j'} A^\alpha_{j'j} y_j + 2\sum_{\tilde{j}'j} y_{j'} B^\alpha_{j'j} x_j\Big]\,, \tag{48}$$

where the tilde over a summation index indicates that the index j_0 has to be left out. Introducing now an $(m = 2n-1)$-dimensional real vector u by

$$u = (x_1, \ldots, x_n, y_1, \ldots, y_{j_0-1}, y_{j_0+1}, \ldots, y_n)\,, \tag{49}$$

one can represent the $n \times n$ hermitean form by an $m \times m$ real quadratic form

$$\widetilde{f}^\alpha(u) = \frac{1}{2}\sum_{l'l=1}^{m} u_{l'} \widetilde{F}^\alpha_{l'l} u_l\,, \tag{50}$$

where the $m \times m$ matrix $\widetilde{F}^\alpha$ is given by

$$\widetilde{F}^\alpha = \begin{pmatrix} A^\alpha & (\widetilde{B}^\alpha)^T \\ \widetilde{B}^\alpha & \widehat{A}^\alpha \end{pmatrix}. \tag{51}$$

Here $\widetilde{B}^\alpha$ is obtained from B^α by canceling the j_0-th row, and $\widehat{A}^\alpha$ from A^α by canceling the j_0-th row and column. Thus $\widetilde{B}^\alpha$ is an $(n-1) \times n$ matrix and $\widehat{A}^\alpha$ an $(n-1) \times (n-1)$ matrix.

Now, for checking the completeness of a chosen set of $2n-1$ observables one has to construct the $m \times m$ corresponding matrices $\widetilde{F}^\alpha$, and then one builds from their columns for all possible sets $\{k_1, \ldots, k_m;\, k_\alpha \in \{1, \ldots, n\}\}$ the matrices

$$\widetilde{W}(k_1, \ldots, k_m) = \begin{pmatrix} \widetilde{F}^1_{1k_1} & \cdots & \widetilde{F}^m_{1k_m} \\ \vdots & & \vdots \\ \widetilde{F}^1_{mk_1} & \cdots & \widetilde{F}^m_{mk_m} \end{pmatrix}. \tag{52}$$

Note that the k_α need not be different. If at least one of the determinants of $\widetilde{W}(k_1, \ldots, k_m)$ is nonvanishing then one has a complete set.

Now we will apply this criterion for the selection of complete sets to the case of deuteron photo- and electrodisintegration. The total number of T-matrix elements for electrodisintegration is $3 \times 3 \times 4 = 36$ which is reduced by parity conservation to $n = 18$. Of these, 6 are associated with the charge or longitudinal current density component while the remaining 12 belong to the transverse current density components. Only the latter appear in photodisintegration. In order to apply our criterion, one first has to construct the matrices $\widetilde{F}$ which represent the structure functions as hermitean forms in the reaction matrix elements as

$$f^{(\prime)\,IM\pm}_\alpha(X) = \sum_{j'j} t^*_{j'} \widetilde{F}^{(\prime)\,IM\pm,\,\alpha}_{j'j}(X)\, t_j\,. \tag{53}$$

According to (8) through (13) one needs the matrix representation of

$$\mathcal{U}^{\lambda'\lambda IM}_X = \sum_{j'j} t^*_{j'} \widetilde{C}^{IM\lambda'\lambda}_{j'j}(X) t_j\,, \tag{54}$$

which can be read off from Eqs. (24) and (34) yielding with $X = (x_{\alpha'} x_\alpha)$

$$\widetilde{C}^{IM\lambda'\lambda}_{j'j}(X) = \sum_{\tau'\nu'\tau\nu} s^{\tau'\nu'}_{\alpha'} s^{\tau\nu}_\alpha\, C^{m_1' m_2' \lambda_d'}_{m_1 m_2 \lambda_d}(\tau'\nu'\tau\nu IM)\,, \tag{55}$$

where the labeling is to be understood as $j^{(\prime)} = (m_1^{(\prime)}, m_2^{(\prime)}, \lambda^{(\prime)}, \lambda_d^{(\prime)})$. Detailed expressions of the $\widetilde{C}^{IM\lambda'\lambda}(X)$'s for several representations are easily obtained from the expressions listed in Appendix C. Then the the $\widetilde{F}$'s are given in terms of the $\widetilde{C}$'s as

$$\widetilde{F}^{IM,\,L}_{j'j}(X) = \frac{2}{1+\delta_{M0}} i^{\bar{\delta}^X_I}\, \widetilde{C}^{IM00}_{j'j}(X)\,, \tag{56}$$

$$\widetilde{F}^{IM,\,T}_{j'j}(X) = \frac{2}{1+\delta_{M0}} i^{\bar{\delta}^X_I} \left[\widetilde{C}^{IM11}_{j'j}(X) + (-)^{\bar{\delta}^X_I} \left(\widetilde{C}^{IM11}_{j'j}(X)\right)^*\right], \tag{57}$$

$$\begin{aligned}\widetilde{F}^{IM\pm,\,LT}_{j'j}(X) = \frac{2}{1+\delta_{M0}} i^{\bar{\delta}^X_I} \Big[&\left(\widetilde{C}^{IM01}_{j'j}(X) \pm (-)^{I+M+\delta_{X,\,B}} \widetilde{C}^{I-M01}_{j'j}(X)\right) \\ &+(-)^{\bar{\delta}^X_I} \left(\widetilde{C}^{IM01}_{j'j}(X) \pm (-)^{I+M+\delta_{X,\,B}} \widetilde{C}^{I-M01}_{j'j}(X)\right)^*\Big],\end{aligned} \tag{58}$$

$$\widetilde{F}^{IM\pm,\,TT}_{j'j}(X) = \frac{2}{1+\delta_{M0}} i^{\bar{\delta}^X_I} \left(\widetilde{C}^{IM-11}_{j'j}(X) \pm (-)^{I+M+\delta_{X,\,B}} \widetilde{C}^{I-M-11}_{j'j}(X)\right), \tag{59}$$

$$\widetilde{F}'^{IM,\,T}_{j'j}(X) = \frac{2}{1+\delta_{M0}} i^{1+\bar{\delta}^X_I} \left[\widetilde{C}^{IM11}_{j'j}(X) - (-)^{\bar{\delta}^X_I} \left(\widetilde{C}^{IM11}_{j'j}(X)\right)^*\right], \tag{60}$$

$$\begin{aligned}\widetilde{F}'^{IM\pm,\,LT}_{j'j}(X) = \frac{2}{1+\delta_{M0}} i^{\bar{\delta}^X_I} \Big[&\left(\widetilde{C}^{IM01}_{j'j}(X) \pm (-)^{I+M+\delta_{X,\,B}} \widetilde{C}^{I-M01}_{j'j}(X)\right) \\ &-(-)^{\bar{\delta}^X_I} \left(\widetilde{C}^{IM01}_{j'j}(X) \pm (-)^{I+M+\delta_{X,\,B}} \widetilde{C}^{I-M01}_{j'j}(X)\right)^*\Big].\end{aligned} \tag{61}$$

It is convenient to arrange the labeling of the t-matrix elements in such a way that the longitudinal ones belong to $j = 1, \ldots, 6$ and the transverse ones to $j = 7, \ldots, 18$. Thus the general structure of these matrices is then

$$\widetilde{F}^{\alpha} = \begin{pmatrix} A^{\alpha} & C^{\alpha} \\ (C^{\alpha})^{\dagger} & B^{\alpha} \end{pmatrix}, \tag{62}$$

where A^{α} is a (6×6)-matrix, C^{α} a (6×12)-matrix, and B^{α} a (12×12)-matrix. In particular one has

$$\widetilde{F}^{L} = \begin{pmatrix} A^{L} & 0 \\ 0 & 0 \end{pmatrix}, \; \widetilde{F}^{(\prime)\,T/TT} = \begin{pmatrix} 0 & 0 \\ 0 & B^{(\prime)\,T/TT} \end{pmatrix}, \text{ and } \widetilde{F}^{(\prime)\,LT} = \begin{pmatrix} 0 & C^{(\prime)\,LT} \\ (C^{(\prime)\,LT})^{\dagger} & 0 \end{pmatrix}. \tag{63}$$

The structure of these matrices is such that the longitudinal (L) and the transverse (T, TT) observables are decoupled filling separated 6×6- and 12×12-submatrices, respectively, whereas the LT-type observables are represented by 18×18-matrices. These features offer various kinds of strategies for selecting complete sets.

(i) One may independently select complete sets of observables for the longitudinal and transverse cases. In other words, one may choose a set of 11 longitudinal structure functions for a check of completeness, and analogously 23 transverse structure functions. With respect to the latter, one has in view of the linear relations between the T- and the TT^{+}-type and between the T'- and TT^{-}-type observables different choices, taking either T- and T'-type or $TT^{\pm}$-type observables or even mixing different types of observables. The missing relative phase between the longitudinal and transverse t-matrix elements can then be provided by any LT-observable. The advantage of this approach is that in this way one automatically obtains complete sets of observables for the case of photodisintegration as well, namely the transverse ones.

(ii) Again one may start with a selection of 11 longitudinal structure functions yielding the longitudinal t-matrix elements. But then instead of choosing transverse observables, one may directly choose 24 linearly independent LT-type observables which then constitute a simple system of linear equations for the missing transverse matrix elements, because the longitudinal ones are then known from the first step.

(iii) Complimentary to case (ii) one may start with a selection of 23 transverse observables taking one of the alternatives listed in (i). Then a proper set of 12 LT-type observables should provide a set of linear equations from which the missing longitudinal t-matrix elements can be obtained.

(iv) An alternative to the foregoing procedures would be a selection of 35 structure functions of LT-type. However, in this case the completeness check would be much more involved due to the considerably higher dimension of the determinants to be checked.

The question which of these strategies is more advantageous will depend on the experimental conditions. Often L- and T-type structure functions are easier to determine in an experiment although the required Rosenbluth separation introduces some unwanted complication. In view of the fact that the strategies (i) through (iii) require the determination of either L- or T-type observables or both we will consider exclusively in the following analysis the question of complete sets for longitudinal and transverse structure functions.

The longitudinal case has already been discussed in detail in [1]. We will briefly summarize the main result. For the analysis of possible complete sets we had chosen the helicity basis. Taking into account the symmetry property of the t-matrix we have used for the labeling of the six independent longitudinal matrix elements the ones listed in Table VII. Allowing general choices for $(k_1, \ldots, k_{11})$, we found that there is only a very weak restriction on the possible sets. In fact one may select any set, which does not include more than eight observables of the type X^{10} and X^{22} of the set of linearly independent observables chosen. They were listed explicitly for $X \in \{1, xx, xz, y_1, x_1, x_2, z_1, z_2\}$ in Table 5 of [1]. As mentioned in [1], this is most easily seen by looking at the structure of the matrices $\widetilde{F}^{(\prime)\,IM\pm,\,\alpha}(X)$ associated with each observable (see (53)) in the helicity basis. But this feature is independent of the basis chosen for the representation of the t-matrices.

For the transverse observables one can proceed in an analogous way. The independent helicity matrix elements in the helicity basis are listed in Table VIII. Again with respect to the general question of a complete set of observables one finds the general statement, that one may pick any set of 23 observables from the chosen set of linearly independent ones with the only restriction, that not more than 16 should be of the type $X^{(\prime)\,10}$ and $X^{(\prime)\,22}$.

In Ref. [1] we simulated an experimental study for the determination of the longitudinal t-matrix elements of the helicity basis from a given set of "measured" observables whose numerical values were taken from a calculation. Various complete sets were selected and the arising system of 11 nonlinear equations for the t-matrix elements was solved. Since the solutions are not unique we had to calculate additional observables, henceforth called "check observables" , taking as input the obtained solutions for the t-matrix elements and compare them to their "measured" values. For the arbitrarily chosen kinematics (internal excitation energy $E_{np} = 100$ MeV, momentum transfer $q^2_{c.m.} = 5$ fm^{-2}, various np angles θ_{np}) we found that one of the considered complete sets was particularly suitable (first set of Table 6 in Ref. [1]). In this case only one additional check observable ($f_L^{10}(x_2)$) was sufficient to determine the correct solution. In the present work we have extended this simulation to a somewhat more realistic experimental situation using the same kinematics ($\theta_{np} = 50$ degrees) again and taking the same specific set but allowing for errors in the measured observables. The size of the error is chosen in two different ways (cases A and B).

For case A we have assumed a statistical error of 10 % for any of the eleven observables (standard deviation $\sigma(f_L^{IM}(X)) = 0.1 f_L^{IM}(X)$). We varied each of the 11 observables randomly, subject to the restriction that the standard deviation of each observable was as given above. A statistically correct randomization procedure was used. We note in passing that in varying the observables one has to pay attention to the fact that they have to fulfill certain boundary conditions (see Appendix D). With these randomly assigned values we have solved again the system of equations and then calculated from the solutions the check observable. If the value of the check observable did not differ more than 10 % from its measured value the solution was accepted. We repeated this procedure 10^5 times obtaining about 1500 accepted solutions. For these successful solutions we have calculated the mean values and standard deviations (experimental errors) for the 11 real and imaginary parts of the t-matrix elements. We had chosen $\Im m(t_1) = 0$. The results are shown in Tables X and XI. Though the mean values come quite close to the correct values of the t-matrix elements (average deviation about 10 %) the standard deviations from the mean values are on the average 44 % and thus the experimental error would be quite large. We have tried to improve our results by considering in addition a second check observable ($f_L^{22}(y_1)$). In this case the number of accepted solutions is reduced to about 400 and the results were much better. In fact we found an average deviation from the true value of 6.5 %. In addition the experimental error came down to an average value of 25 % which, however, is still quite sizable.

One may argue that case A is not very realistic, since we had assumed the same relative error for all observables independent of their size. However, observables with large values can probably be measured with a higher precision than observables with small values. Thus for case B we made a different choice. We assumed that the largest observable can be determined with a relative error of 1 % and then we take the resulting absolute uncertainty for all the other observables as their absolute error. For our smallest observable this led to a relative error of about 40 %. With one check observable we found about 1300 accepted solutions and obtained average values very close to the true values (average deviation 1.0 %), but the experimental error is on the average 22 % and thus still quite large. Considering two check observables for case B also leads to an important improvement. With the 440 successful solutions we found an average experimental error of only 4.0 %. The average deviation of the mean values from the exact values is similar as before (1.2 %).

Our simulation of an experimental situation shows that one can get rather reliable results for the t-matrix elements even if experimental errors are taken into account. The results can be greatly improved if additional check observables are considered. For our case it was sufficient to consider two such observables. If on the other hand one uses no check observables at all one gets rather unreliable results since other types of solutions of the nonlinear system of equations are mixed in. In fact, performing our simulation without any check observable leads to large experimental errors (average error more than 100 %) and also to strong average deviations of the mean values from the true values of the t-matrix elements (about 50 %).

We also made a similar study for the determination of the transverse t-matrix elements from observables, but without

introducing experimental errors. However, the transverse case is much more complicated than the longitudinal one due to the higher dimensionality (12 instead of 6 complex t-matrix elements), since one has to solve a system of 23 nonlinear equations. We have used two different complete sets, which are listed in Table XII. The first set has been chosen arbitrarily considering only target asymmetries and observables with proton polarization components P_x and P_y. On the contrary, the second set was chosen using one of the sets obtained from the inversion of the bilinear t-matrix expressions as discussed in the next section. In both cases we took 4 additional check observables, namely $f_T^{10}(x_2)$, $f_T^{11}(x_2)$, $f_T'^{00}(x_2)$, and $f_T^{11}(z_2)$ for the first set and $f_T^{22}(1)$, $f_T'^{00}(x_1)$, $f_T^{10}(x_2)$, and $f_T^{11}(x_2)$ for the second set. Our numerical method to solve the system of equations asks for starting values for the 23 real and imaginary parts of the t-matrix elements. We have determined these starting values on a random basis. For both complete sets we made 10^6 trials. In order to classify the solutions we have evaluated the check observables from the solution. Then we summed the squares of their differences to their true values and took it as a measure for the quality of the solution. The best solutions of the first set led to rather good results for the real parts of the t-matrix elements, while the smaller imaginary parts were not so well described. Thus no correct solution had been found with 10^6 trials. Of course one could increase the number of trials or search for a more efficient choice for the starting values. For the second complete set the situation was much better. Though we did not find a completely correct solution with 10^6 trials, the best solution came extremely close to the correct solution. Ten of the 23 real and imaginary parts of the t-matrix elements were determined better than 1 % and most of the rest also with a rather good relative precision. Larger deviations were only found in three cases, but these concern extremely small matrix elements which are 10^2 - 10^3 times smaller than the largest t-matrix element. Thus the solution could be considered to be practically correct, and this shows that in principle the method works also for the transverse case.

IV. DERIVATION OF BILINEAR T-MATRIX EXPRESSIONS

One can also derive a direct solution of the reaction matrix elements in terms of observables, because one can express all bilinear forms $t^*_{j'}t_j$ as linear combinations of the structure functions $f_\alpha^{(\prime)IM}(X)$, i.e.,

$$t^*_{j'}t_j = T_{j'j}[f_\alpha^{(\prime)IM}(X)]\,. \tag{64}$$

This is possible because the spin operators representing the various polarization degrees of freedom form a complete basis of operators in spin space. An explicit solution has been reported in [3] for the case of deuteron photodisintegration. In order to extend this case to electrodisintegration, we invert first the relations in (8) through (13) yielding the following expressions for $M \geq 0$ in

$$\mathcal{U}_X^{00\,IM} = \frac{1}{2}(1+\delta_{M0})\,i^{-\bar\delta_I^X}\,f_L^{IM}(X)\,, \tag{65}$$

$$\mathcal{U}_X^{11\,IM} = \frac{1}{4}(1+\delta_{M0})\,i^{-\bar\delta_I^X}\left(f_T^{IM}(X) - i\,f_T'^{IM}(X)\right), \tag{66}$$

$$\mathcal{U}_X^{01\,IM} = \frac{1}{8}(1+\delta_{M0})\,i^{-\bar\delta_I^X}\left(f_{LT}^{IM+}(X) + f_{LT}^{IM-}(X) - i\,(f_{LT}'^{IM+}(X) + f_{LT}'^{IM+}(X))\right), \tag{67}$$

$$\mathcal{U}_X^{01\,I-M} = \frac{(-)^M}{8}(1+\delta_{M0})\,i^{\bar\delta_I^X}\left(f_{LT}^{IM+}(X) - f_{LT}^{IM-}(X) - i\,(f_{LT}'^{IM+}(X) - f_{LT}'^{IM+}(X))\right), \tag{68}$$

$$\mathcal{U}_X^{-11\,IM} = \frac{1}{4}(1+\delta_{M0})\,i^{-\bar\delta_I^X}\left(f_{TT}^{IM+}(X) + f_{TT}^{IM-}(X)\right), \tag{69}$$

$$\mathcal{U}_X^{-11\,I-M} = \frac{(-)^M}{4}(1+\delta_{M0})\,i^{\bar\delta_I^X}\left(f_{TT}^{IM+}(X) - f_{TT}^{IM-}(X)\right). \tag{70}$$

The other $\mathcal{U}$'s not listed above can be obtained from the foregoing ones by use of the symmetry relations in (42).

The $\mathcal{U}_X^{\lambda'\lambda IM}$'s in turn are given as linear forms in $t^*_{j'}t_j$ of the reduced t-matrix elements which one can invert so that any $t^*_{j'}t_j$ can be expressed as linear superposition of the $\mathcal{U}_X^{\lambda\lambda' IM}$'s

$$t_{j'}^{R_f R_d\,*}t_j^{R_f R_d} = \sum_{IM}\sum_{\alpha',\alpha=0}^{3}\widetilde{T}_{j'j}^{IM\alpha'\alpha}\,\mathcal{U}_{\alpha'\alpha}^{\lambda'\lambda IM}\,. \tag{71}$$

The inversion is easily achieved. Starting from (24) and (34) and using the orthogonality relation of (41) in conjunction with (21), one obtains for the general representation ($j^{(\prime)} = (m_1^{(\prime)}, m_2^{(\prime)}, \lambda^{(\prime)}, \lambda_d^{(\prime)})$)

$$\widetilde{T}^{IM\alpha'\alpha}_{j'j} = \frac{1}{12} \sum_{\tau'\nu'\tau\nu} (C^{m_1' m_2' \lambda_d'}_{m_1 m_2 \lambda_d}(\tau'\nu'\tau\nu IM))^* \, c^{\alpha'}_{\tau'\nu'} \, c^{\alpha}_{\tau\nu} \,, \tag{72}$$

where for the uncoupled basis $(m_1, m_2) = (\lambda_p, \lambda_n)$, and the matrix elements are labeled by $j^{(\prime)} = (\lambda_p^{(\prime)}, \lambda_n^{(\prime)}, \lambda^{(\prime)}, \lambda_d^{(\prime)})$, whereas for the coupled basis $(m_1, m_2) = (s, m_s)$ and $j^{(\prime)} = (s^{(\prime)}, m_s^{(\prime)}, \lambda^{(\prime)}, m_d^{(\prime)})$. More explicit expressions for the normal helicity, hybrid and standard bases can be obtained with the help of Appendix C.

The bilinear relations in (71) can now be exploited in various ways. One possibility is to choose a fixed matrix element, say t_{j_0}, as real and positive. Then all other matrix elements t_j with $j \neq j_0$ are uniquely determined relative to t_{j_0} and given as linear forms of appropriate structure functions [3]

$$t_j = \frac{1}{t_{j_0}} T_{j_0 j}[f_\alpha^{(\prime) IM\pm}(X)] \,. \tag{73}$$

Finally, for the determination of the missing matrix element t_{j_0} one has to choose only one additional structure function, say f_0, which has the general form (see (53))

$$f_0 = \sum_{j'j} t^*_{j'} \tilde{F}_{j'j} t_j \,. \tag{74}$$

Inserting t_j from (73) one finds

$$t_{j_0} = \sqrt{\frac{\sum_{j'j} T_{j'j_0} \tilde{F}_{j'j} T_{j_0 j}}{f_0}} \,. \tag{75}$$

However, proceeding in this way, one needs in general a much larger number of observables for the complete determination of the t-matrix than the required minimal number of $2n-1$ of a complete set of a n-dimensional t-matrix.

A more general strategy which leads in general to a smaller number of necessary observables is to study first all interference terms with respect to the question, which and how many observables are involved, because a closer inspection of the explicit expressions reveals, that in general they can be divided into subgroups which are governed by a restricted number of observables. In order to visualize this grouping we have devised a graphical representation. To this end we assemble the numbers "1" through "n" by points on a circle and represent a term $t^*_{j'} t_j$ by a straight line joining the points "j" and "j'". Interference terms belonging to the same group are then represented by the same type of lines as is demonstrated below.

As next step one has to choose from the total number of interference terms $t^*_{j'} t_j$ with $j' > j$ which is $\frac{1}{2} n(n-1)$ – not counting $t^*_{j'} t_j$ with $j' < j$, because $(t^*_{j'} t_j)^* = t^*_j t_{j'}$ – a set of $n-1$ independent interference terms. The meaning of "independent interference terms" can be explained most easily by a graphical representation. Assembling again the numbers as before, we consider first a set of connected interference terms, which means that they generate a pattern of connected lines so that any point belonging to one of the considered interference terms is connected to any other point of the set either directly or via k other points of that set. In such a set any matrix element $t_{j'}$ can be expressed in terms of any other matrix element t_j of that set by one of the two forms

$$t_{j'} = \begin{cases} \frac{T_{j_1 j'}}{T_{j_1 j_2}} \frac{T_{j_3 j_2}}{T_{j_3 j_4}} \cdots \frac{T_{j_{k-2} j_{k-3}}}{T_{j_{k-2} j_{k-1}}} \frac{T_{j_k j_{k-1}}}{T_{j_k j}} \, t_j & \text{for } k \text{ odd}, \\ \frac{T_{j_1 j'}}{T_{j_1 j_2}} \frac{T_{j_3 j_2}}{T_{j_3 j_4}} \cdots \frac{T_{j_{k-3} j_{k-4}}}{T_{j_{k-3} j_{k-2}}} \frac{T_{j_{k-1} j_{k-2}}}{T_{j_{k-1} j_k}} \frac{T_{j j_k}}{t^*_j} & \text{for } k \text{ even}, \end{cases} \tag{76}$$

depending on whether the number k of intermediate points connecting j' with j via the points j_1 through j_k is odd or even. The proof of these equations is easily established by considering the simplest two cases of connecting two points via one and two intermediate points. For one intermediate point j_1 connecting j' with j one finds

$$t_{j'} = \frac{T_{j_1 j'}}{T_{j_1 j}} \, t_j \,, \tag{77}$$

and for two intermediate points j_1 and j_2

$$t_{j'} = \frac{T_{j_1 j'}}{T_{j_1 j_2}} \frac{T_{j j_2}}{t^*_j} \,. \tag{78}$$

Iteration of these cases yields obviously (76).

If one has a closed loop with an even number of points then one finds from (76) for $j' = j$ and k odd the following condition

$$\frac{T_{j_1 j}}{T_{j_1 j_2}} \frac{T_{j_3 j_2}}{T_{j_3 j_4}} \cdots \frac{T_{j_{k-2} j_{k-3}}}{T_{j_{k-2} j_{k-1}}} \frac{T_{j_k j_{k-1}}}{T_{j_k j}} = 1 \,, \tag{79}$$

or equivalently

$$T_{j_k j_{k-1}} T_{j_{k-2} j_{k-3}} \cdots T_{j_3 j_2} T_{j_1 j} = T_{j_1 j_2} T_{j_3 j_4} \cdots T_{j_{k-2} j_{k-1}} T_{j_k j} \,, \tag{80}$$

which means that in such a closed loop any interference term is completely determined by the other remaining interference terms of that loop. This condition thus constitutes a relation between the participating observables. On the other hand for a closed loop through an odd number of points, all participating t-matrix elements are completely determined up to one arbitrary phase because for $j' = j$ and k even (76) yields

$$|t_j|^2 = \frac{T_{j_1 j}}{T_{j_1 j_2}} \frac{T_{j_3 j_2}}{T_{j_3 j_4}} \cdots \frac{T_{j_{k-3} j_{k-4}}}{T_{j_{k-3} j_{k-2}}} \frac{T_{j_{k-1} j_{k-2}}}{T_{j_{k-1} j_k}} \, T_{j j_k} \,. \tag{81}$$

This means one may choose one matrix element of that loop as real and non-negative, fix its modulus according to (81) and then all other matrix elements of the loop are uniquely determined.

Now a set of $n-1$ independent interference terms is represented by a pattern of $n-1$ lines in such a fashion that (i) each of the n points is endpoint of at least one line, and (ii) each point is connected to all other points not necessarily in a direct manner but via intermediate points. It is obvious that in such a pattern no closed loops can be present, because one cannot construct a closed loop with $n-1$ lines such that all n points are connected. Then all matrix elements can be expressed by one arbitrarily chosen matrix element, say t_{j_0} according to (76). In order to fix the remaining undetermined matrix element t_{j_0} one has to choose one additional observable f_0. From the form (74) one obtains in general an equation of the type

$$f_0 = a + b\,|t_{j_0}|^2 + c\,|t_{j_0}|^{-2} \,, \tag{82}$$

from which t_{j_0} can be obtained, although not uniquely in general. The ideal situation would be such that one finds $n-1$ independent interference terms each of them represented by only two observables. Because in this case one employs just $2n-1$ observables. On the other hand analyzing the grouping of observables mentioned above, one will in general not find such a situation, either the number of observables for a set of $n-1$ independent interference terms is larger than $2n-2$, or the grouping is such, that the choice of $n-1$ independent interference terms involves observables which govern at least one additional interference term leading to one or several closed loops.

We will now illustrate such an analysis for the case of the longitudinal matrix elements. In evaluating the bilinear expressions for this case, one has to use the linear relations between structure functions [4] in order to have only the linearly independent ones. According to Table 6 of [4] we have chosen for the A-type observables $X = 1, y(1), xz, zz$ and for the B-type ones $X = x(1), x(2), z(1), z(2)$. We show in Fig. 2 for the helicity basis the graphical representation of the various groups of structure functions into which the interference terms divide. They are listed explicitly in Table III. One readily notes that altogether there are two groups, panel (c), each containing four observables and each determining two different interference terms, one group (a) with six observables determining three interference terms of which one interference term, T_{12}, contains only four observables and finally two groups (b) and (d) with eight observables which each determine four independent interference terms.

The resulting grouping and nomenclature for the hybrid basis is shown in Fig. 3 and Table IV, respectively. The pattern looks similar to the helicity basis, though the number and type of observables involved are different. One finds in panel (a) two groups each containing six observables and each determining two different interference terms. Furthermore, there are three groups of eight observables. Two of them, (b) and (d), determine four independent interference terms. They both involve the same type of single nucleon polarization components which differ only with respect to the particle number. The third panel (c) determines only three independent interference terms, of which one, T_{21}, involves only six observables.

In Fig. 4 and Table V we show and explain the nomenclature for the grouping for the standard basis. The evolving pattern differs distinctly from the foregoing ones. First of all, one has two groups of four, each determining only one interference term (panel (a)). In panel (b), we show a group of ten observables determining five interference terms containing a closed loop of four points and a disconnected line, i.e., a disconnected interference term. The latter is given by a subgroup of four observables as is indicated by the dashed line. Then there are two groups of eight observables for four interference terms in the panels (c) and (d). In each of these groups there are two connected interference terms which need all eight observables. Disconnected from these two, one notes two other connected interference terms, each of which is determined by disjunct groups of four, indicated by dashed and dotted lines.

Other possible groups of observables are found by studying various rotations of the initial and final spin states. We have chosen rotations carrying the quantization axis into the x-axis ($R_x = R(0, \pi/2, 0)$) and the y-axis ($R_y = R(\pi/2, \pi/2, -\pi/2)$). We found that rotating only the final uncoupled spin states into the y-axis, i.e., $R_f = R_y$ and $R_d = R(0, 0, 0)$, was most interesting. We show this case as our last example in Fig. 5 supplemented by Table VI. The pattern looks again like the one for the helicity basis. However, the grouping for the transformed basis is quite different. One finds six groups of four observables, each determining two interference terms, and one group of six observables for three independent interference terms, of which one, T_{12}, is given by four observables alone.

These patterns can now be used to select sets of observables for a complete determination of the t-matrix elements. Let us first consider the case of the helicity basis. It is obvious that one should take one of the groups of eight observables in panels (b) or (d) of Fig. 2 which fix four matrix elements in terms of two. Then one can choose as additional group of four from panel (c) the dashed line group because, taking the full line group of panel (c), one would obtain two disconnected 3-point loops. Thus twelve observables lead to five complex t-matrix elements. Furthermore, since such a choice leads to a closed loop of an even number of points (6), one has an additional complex condition between the observables, eliminating two and thus leaving ten observables. In order to fix the last matrix element which can be chosen real and non-negative, one needs only one additional observable. The solution, however, could still contain an ambiguity (see (82)).

The largest variety of possible selections of observables is offered by the case for the rotated basis in Fig. 5. First one may take such combinations of two of the groups of four observables determining four independent interference terms so that one avoids any closed loops. Then four matrix elements are given as function of the remaining two involving eight observables. The missing fifth interference term can be provided by choosing one of the remaining three groups of four observables with the only restriction that one should avoid two disconnected closed loops of three points. Obviously, one will then encounter loops of four or six points so that of the twelve observables involved two can be eliminated leaving one with ten observables.

Taking into account the one remaining required observable, say f_L, one obtains in this way various groups of eleven observables, which allow one to determine the longitudinal matrix elements up to discrete ambiguities whose resolution needs additional observables [1]. Alternatively one could use for the missing fifth interference term the one containing six observables in Fig. 5. In that case one could find two closed loops resembling two conditions between observables. The possible scenarios are discussed explicitly in the Appendix E where we also display the various cases diagrammatically in Figs. 6 and 7.

The transverse case is more involved due to the larger number of t-matrix elements. For this reason, we will not display the grouping of observables for all four bases as we did for the longitudinal matrix elements, but consider only two of them, the helicity basis and the transformed one. As independent matrix elements we have chosen those with $\lambda = 1$ for the photon helicity. The matrix elements are numbered $7, \ldots, 18$ as listed in Table VIII of Appendix E. The resulting diagrammatic representation of the grouping of observables is shown in Fig. 8. We find for both cases identical patterns for the various groups although with different observables (see Tables XVI and XVII of Appendix E). In both cases we find groups of eight observables determining four interference terms (dashed lines), of twelve observables determining six interference terms (dash-dot-dot lines) and of sixteen observables for eight terms (solid lines). Combined properly according to the types of observables, they form highly symmetrical patterns. In panel (a) one has four disconnected loops of three points, whereas in the other three panels one notices a separation into two disconnected groups of six points building one closed loop of six points and containing in addition various interconnections. One then has to find proper combinations of these various groups such that one can express all matrix elements in terms of one. For the transverse matrix elements this task is more involved than the longitudinal case. A detailed analysis, however, shows that it is possible to find a variety of patterns containing 36 observables, which allow a unique determination of all matrix elements as a function of an arbitrarily chosen one. Moreover, the number of observables can be reduced to 22, the minimal number required, by exploiting the conditions implied by the various closed loops appearing in the diagrams, This will be discussed in greater detail for one case in the Appendix E.

V. SUMMARY AND CONCLUSION

In this work we have discussed various strategies for the selection of complete sets of polarization observables to be used for a complete determination of all 12, respectively 18 independent t-matrix elements for photo- and electrodisintegration of the deuteron. Such sets consist of 23, respectively 35 observables. Two different methods have been considered:

(i) Application of a newly developed criterion allowing a check of whether an arbitrarily chosen set of observables is complete, and

(ii) construction of an explicit solution for the t-matrix elements as function of observables by explicit inversion of the hermitean forms by which the observables are given in terms of the t-matrix elements.

The first method is certainly much more versatile in so far as one has a much greater variety of choices whereby a choice may be governed by the question of easy access of the corresponding observables in an experiment. In a numerical simulation we have studied the practical applicability and found quite satisfactory results if a few additional check observables are considered which allow one to eliminate the inherent discrete ambiguities. But the second method has its merits, too, because it may allow an explicit analytic solution depending on the choice of basis for the representation of the t-matrix.

ACKNOWLEDGMENT

Parts of this work were done while H.A. and E.L.T. were at the Dipartimento di Fisica of the Università degli Studi di Trento and while H.A. and W.L. were visiting the Saskatchewan Accelerator Laboratory and the Department of Physics of the University of Saskatchewan, Saskatoon. In all cases the authors thank the respective institutions for their hospitality.

---

[1] H. Arenhövel, W. Leidemann, and E.L. Tomusiak, Nucl. Phys. A **641**, 517 (1998).
[2] H. Arenhövel, Few-Body Syst. **4**, 55 (1988).
[3] H. Arenhövel and K.-M. Schmitt, Few-Body Syst. **8**, 77 (1990).
[4] H. Arenhövel, W. Leidemann, and E.L. Tomusiak, Few-Body Syst. **15**, 109 (1993).
[5] M.E. Rose, Elementary Theory of Angular Momentum (Wiley, New York 1963)
[6] V. Dmitrasinovic and F. Gross, Phys. Rev. **C40**, 2479 (1989)

APPENDIX A: COMPARISON WITH THE FORMALISM OF DMITRASINOVIC AND GROSS

For the comparison with the formalism of Dmitrasinovic and Gross [6], which henceforth we will refer to by DG, we rewrite our expression for the general observable in (1) as follows

$$\begin{aligned}\mathcal{O}(X) = c(k_1^{lab}, k_2^{lab})\Big\{&\rho_L \tilde{f}_L(X) + \rho_T \tilde{f}_T(X) + \rho_{LT}\Big(\tilde{f}^{+}_{LT}(X)\cos\phi - \tilde{f}^{-}_{LT}(X)\sin\phi\Big) \\ &+\rho_{TT}\Big(\tilde{f}^{+}_{TT}(X)\cos 2\phi - \tilde{f}^{-}_{TT}(X)\sin 2\phi\Big) \\ &+h\Big[\rho'_T \tilde{f}'_T(X) + \rho'_{LT}\Big(\tilde{f}'^{-}_{LT}(X)\cos\phi + \tilde{f}'^{+}_{LT}(X)\sin\phi\Big)\Big]\Big\}\,, \end{aligned} \tag{A.1}$$

where we have introduced

$$\tilde{f}^{(\prime)\pm}_{\alpha}(X) = \sum_{I=0}^{2} P^d_I \sum_{M=0}^{I} d^I_{M0}(\theta_d)\, f^{(\prime)IM\,\pm}_{\alpha}(X) \begin{cases} \cos(M\tilde{\phi} - \bar{\delta}^X_I \frac{\pi}{2}) & \text{for } + \\ \sin(M\tilde{\phi} - \bar{\delta}^X_I \frac{\pi}{2}) & \text{for } - \end{cases}, \tag{A.2}$$

with the understanding for $\alpha = L$ and T

$$\tilde{f}^{+}_{L/T}(X) = \tilde{f}_{L/T}(X)\,, \quad \tilde{f}^{-}_{L/T}(X) = 0\,, \tag{A.3}$$

$$\tilde{f}'^{-}_{T}(X) = \tilde{f}'_{T}(X)\,, \quad \tilde{f}'^{+}_{T}(X) = 0\,. \tag{A.4}$$

On the other hand, DG give the general coincidence cross section including target polarization and single outgoing nucleon polarization in the form (see Eq. (30) of DG)

$$\begin{aligned}\frac{d^3\sigma}{dk_2^{lab} d\Omega_e^{lab} d\Omega_{np}^{c.m.}} = \frac{\sigma_M p_{np}}{4\pi M_d}\Big\{&\Big(\frac{W}{M_d}\Big)^2 v_L R_L + v_T R_T + \frac{W}{M_d} v_{TL}\Big(R^{(I)}_{LT}\cos\phi + R^{(II)}_{LT}\sin\phi\Big) \\ &+v_{TT}\Big(R^{(I)}_{TT}\cos 2\phi + R^{(II)}_{TT}\sin 2\phi\Big) + h\Big[v'_T R'_T + \frac{W}{M_d} v'_{TL}\Big(R'^{(II)}_{LT}\cos\phi + R'^{(I)}_{LT}\sin\phi\Big)\Big]\Big\} \end{aligned} \tag{A.5}$$

where we have changed slightly the original notation of DG for $\alpha = T$, LT and $C = I$, II by defining

$$R'^{(C)}_{\alpha} := R^{(C)}_{\alpha'} \,. \tag{A.6}$$

In contrast to DG, here h denotes not only the electron helicity but also the degree of electron polarization, i.e. $|h| \leq 1$. Furthermore, σ_M denotes the Mott cross section, and the kinematic functions $v^{(\prime)}_{\alpha}$ are related to the $\rho^{(\prime)}_{\alpha}$ by

$$\Big(\frac{W}{M_d}\Big)^2 v_L = \frac{2\eta}{Q^2}\rho_L, \quad Q^2 = -q^2 \,, \tag{A.7}$$

$$v^{(\prime)}_{\alpha} = \frac{2\eta}{Q^2}\rho^{(\prime)}_{\alpha} \,, \quad \alpha = T,\, TT \,, \tag{A.8}$$

$$\frac{W}{M_d} v^{(\prime)}_{TL} = -\frac{2\eta}{Q^2}\rho^{(\prime)}_{LT} \,. \tag{A.9}$$

Here $\beta = W/M_d$ expresses the boost from the final state c.m. system, having the invariant mass W, to the laboratory system, because the R's are evaluated in the c.m. system. The observables are divided into two classes (denoted by I and II) and given in the form for $\widetilde{I} \in \{I, II\}$ and with a changed notation from DG's $R^{(\widetilde{I})}_{\alpha(\prime)}(P_j, T_i)$ (see Eq. (79) of DG) to $R^{(\prime)\,(\widetilde{I})}_{\alpha}(X_j, i)$

$$R^{(\prime)\,(\widetilde{I})}_{\alpha} = \sum_{j \in \widetilde{I}} P_{X_j} R^{(\prime)\,(\widetilde{I})}_{\alpha}(X_j) \,, \tag{A.10}$$

with

$$R^{(\prime)\,(\widetilde{I})}_{\alpha}(X_j) = \sum_{i \in \widetilde{I}} T_i R^{(\prime)\,(\widetilde{I})}_{\alpha}(X_j, i) \,, \tag{A.11}$$

where T_i denotes the deuteron polarization parameters in the so-called hybrid basis. According to the tables X through XII of DG, for the observables corresponding to $X = U$ and $X = P_n$ (notation of DG), which are of A-type, one has for class I and $i = 1, \ldots, 5$

$$T_i \in \Big\{U,\, \sqrt{\frac{3}{2}}\, T_{10},\, \frac{1}{\sqrt{2}}\, T_{20},\, \sqrt{3}\, \Re e(T_{22}),\, \sqrt{3}\, \Im m(T_{22})\Big\} \,,$$

and for class II and $i = 6, \ldots, 9$

$$T_i \in \Big\{\sqrt{\frac{3}{2}}\, \Re e(T_{11}),\, \sqrt{\frac{3}{2}}\, \Im m(T_{11}),\, \sqrt{\frac{3}{2}}\, \Re e(T_{21}),\, \sqrt{\frac{3}{2}}\, \Im m(T_{21})\Big\} \,,$$

while for $X = P_s$ and $X = P_l$, which are of B-type, one has the opposite assignment of T_i for classes I and II.

Inserting now (A.7) through (A.9) and (A.10) into (A.5), one finds the correspondence of (1) in terms of the $R^{(\prime)\,(I/II)}_{\alpha}(X_j)$

$$\begin{aligned} \mathcal{O}(X) = c(k_1^{lab}, k_2^{lab})\bar{c}\Big\{ & \rho_L R_L(X) + \rho_T R_T(X) - \rho_{LT}\Big(R^{(I)}_{LT}(X)\cos\phi + R^{(II)}_{LT}(X)\sin\phi\Big) \\ & + \rho_{TT}\Big(R^{(I)}_{TT}(X)\cos 2\phi + R^{(II)}_{TT}(X)\sin 2\phi\Big) \\ & + h\Big[\rho'_T R'_T(X) - \rho'_{LT}\Big(R'^{(II)}_{LT}(X)\cos\phi + R'^{(I)}_{LT}(X)\sin\phi\Big)\Big]\Big\} \,, \end{aligned} \tag{A.12}$$

where

$$\bar{c} = \frac{3\alpha\pi p_{np}}{M_d} \,. \tag{A.13}$$

Comparison with our expression in (A.1) then yields the following correspondence

$$\bar{c}\, R^{(\prime)\,(I/II)}_{\alpha}(X) = s^{(\prime)\,(I/II)}_{\alpha}\, \tilde{f}^{(\prime)\,\pm}_{\alpha}(X) \,, \tag{A.14}$$

where $s_{LT}^{(I)} = s_{TT}^{(II)} = s_{LT}^{\prime\,(I/II)} = -1$ and $s_\alpha^{(\prime)\,(C)} = 1$ otherwise.

Now we will proceed to find the relation between the structure functions $R_\alpha^{(\prime)\,(I/II)}(X_j, i)$ of DG and our $f_\alpha^{(\prime)IM\,\pm}(X)$. To this end, we will introduce first a more compact notation for the R's. According to what has been said above, one finds explicitly for observables of A-type in class I and of B-type in class II, i.e. $X \in A$, $C = I$ and $X \in B$, $C = II$

$$\sum_{i\in C} T_i R_\alpha^{(\prime)\,(C)}(X,i) = R_\alpha^{(\prime)\,(C)}(X,1) + \sqrt{\frac{3}{2}}\, T_{10}\, R_\alpha^{(\prime)\,(C)}(X,2) + \frac{1}{\sqrt{2}}\, T_{20}\, R_\alpha^{(\prime)\,(C)}(X,3) + \sqrt{3}\, \Re e(T_{22})\, R_\alpha^{(\prime)\,(C)}(X,4) + \sqrt{3}\, \Im m(T_{22})\, R_\alpha^{(\prime)\,(C)}(X,5)\,, \tag{A.15}$$

and analogously for observables of A-type in class II and of B-type in class I, i.e. $X \in A$, $C = II$ and $X \in B$, $C = I$

$$\sum_{i\in C} T_i R_\alpha^{(\prime)\,(C)}(X,i) = \sqrt{\frac{3}{2}}\Big(\Re e(T_{11})\, R_\alpha^{(\prime)\,(C)}(X,6) + \Im m(T_{11})\, R_\alpha^{(\prime)\,(C)}(X,7) + \Re e(T_{21})\, R_\alpha^{(\prime)\,(C)}(X,8) + \Im m(T_{21})\, R_\alpha^{(\prime)\,(C)}(X,9)\Big)\,. \tag{A.16}$$

Noting the property

$$(T_{IM})^* = (-)^M T_{I-M}\,, \tag{A.17}$$

one can rewrite (A.15) into the form

$$\sum_{i\in C} T_i R_\alpha^{(\prime)\,(C)}(X,i) = \sum_{IM} \frac{1}{2}(1 + (-)^M) T_{IM} R_\alpha^{(\prime)\,IM(C)}(X)\,, \tag{A.18}$$

where we have defined

$$R_\alpha^{(\prime)\,00(C)}(X) = R_\alpha^{(\prime)\,(C)}(X,1)\,, \tag{A.19}$$

$$R_\alpha^{(\prime)\,10(C)}(X) = \sqrt{\frac{3}{2}} R_\alpha^{(\prime)\,(C)}(X,2)\,, \tag{A.20}$$

$$R_\alpha^{(\prime)\,20(C)}(X) = \frac{1}{\sqrt{2}} R_\alpha^{(\prime)\,(C)}(X,3)\,, \tag{A.21}$$

$$R_\alpha^{(\prime)\,22(C)}(X) = \frac{\sqrt{3}}{2}\Big(R_\alpha^{(\prime)\,(C)}(X,4) - i R_\alpha^{(\prime)\,(C)}(X,5)\Big)\,, \tag{A.22}$$

$$R_\alpha^{(\prime)\,2-2(C)}(X) = (R_\alpha^{(\prime)\,22(C)}(X))^*\,, \tag{A.23}$$

$$\tag{A.24}$$

and correspondingly for (A.16)

$$\sum_{i\in C} T_i\, R_\alpha^{(\prime)\,(C)}(X,i) = \sum_{IM} \frac{1}{2}(1 - (-)^M)\, T_{IM}\, R_\alpha^{(\prime)\,IM(C)}(X)\,, \tag{A.25}$$

with

$$R_\alpha^{(\prime)\,11(C)}(X) = \frac{1}{2}\sqrt{\frac{3}{2}}\Big(R_\alpha^{(\prime)\,(C)}(X,6) - i R_\alpha^{(\prime)\,(C)}(X,7)\Big)\,, \tag{A.26}$$

$$R_\alpha^{(\prime)\,1-1(C)}(X) = -(R_\alpha^{(\prime)\,11(C)}(X))^*\,, \tag{A.27}$$

$$R_\alpha^{(\prime)\,21(C)}(X) = \frac{1}{2}\sqrt{\frac{3}{2}}\Big(R_\alpha^{(\prime)\,(C)}(X,8) - i R_\alpha^{(\prime)\,(C)}(X,9)\Big)\,, \tag{A.28}$$

$$R_\alpha^{(\prime)\,2-1(C)}(X) = -(R_\alpha^{(\prime)\,21(C)}(X))^*\,. \tag{A.29}$$

For later purposes we note the property

$$(R_\alpha^{(\prime)\,IM(C)}(X))^* = (-)^M R_\alpha^{(\prime)\,I-M(C)}(X)\,. \tag{A.30}$$

Furthermore, for the comparison with our f's it is more convenient to use instead of "I" and "II" for the two classes the notation "+" and "−", respectively. This then results in the compact relation

$$\begin{aligned} R_\alpha^{(\prime)\,\pm}(X) &= \sum_i T_i\, R_\alpha^{(\prime)\,(I/II)}(X,i) \\ &= \sum_{IM} \frac{1}{2}(1 \pm (-)^{M+\delta_{X,B}})\, T_{IM}\, R_\alpha^{(\prime)\,IM\,\pm}(X)\,, \end{aligned} \tag{A.31}$$

and the relation in (A.14) reads as

$$\bar{c} R_\alpha^{(\prime)\,\pm}(X) = s_\alpha^{(\prime)\,\pm} \tilde{f}_\alpha^{(\prime)\pm}(X)\,, \tag{A.32}$$

where $s_\alpha^{(\prime)\,\pm}$ is analogously defined as $s_\alpha^{(\prime)\,(C)}$, i.e. $s_{LT}^{+} = s_{TT}^{-} = s_{LT}^{\prime\pm} = -1$ and $s_\alpha^{(\prime)\,\pm} = 1$ otherwise.

Next, we have to express the polarization parameters T_{IM} of DG, which refer to the transversity basis, by our polarization parameters (P_I^d, θ_d, ϕ_d). DG describe first the deuteron density matrix by parameters $\widetilde{T}_{IM}$ which refer to a coordinate system associated with the reaction plane having the z-axis along the deuteron momentum. The relation of the T_{IM} in the transversity basis to the $\widetilde{T}_{IM}$ is obtained by two transformations, first one to the helicity basis

$$\widetilde{T}_{IM} \longrightarrow (-)^{I+M} \widetilde{T}^*_{IM} = (-)^I \widetilde{T}_{I-M}\,, \tag{A.33}$$

and then in a second step to the transversity basis by a rotation by $-\pi/2$ around the x-axis

$$(-)^I \widetilde{T}_{I-M} \longrightarrow \sum_{M'} D^{I\,*}_{MM'}(\pi/2, \pi/2, -\pi/2)(-)^I \widetilde{T}_{I-M'}\,, \tag{A.34}$$

with D-matrices in the convention of Rose [5], giving

$$T_{IM} = \sum_{M'} i^{M-M'} d^I_{MM'}(\frac{\pi}{2})\,(-)^{I+M'} \widetilde{T}^*_{IM'}\,. \tag{A.35}$$

Furthermore, since our polarization parameters refer to a coordinate system associated with the scattering plane, we find

$$\widetilde{T}_{IM} = P_I^d e^{-iM\tilde{\phi}} d^I_{M0}(\theta_d)\,. \tag{A.36}$$

Thus we have

$$T_{IM} = (-)^I P_I^d \sum_{M'} i^{M+M'} d^I_{MM'}(\frac{\pi}{2}) e^{iM'\tilde{\phi}} d^I_{M'0}(\theta_d)\,. \tag{A.37}$$

Inserting this expression into (A.31) and reordering it, one finds

$$\begin{aligned} R_\alpha^{(\prime)\,\pm}(X) &= \sum_{IM} (-)^I P_I^d\, A_{IM}\, B_\alpha^{(\prime)\,IM\,\pm}(X) \\ &= \sum_I (-)^I P_I^d \sum_{M=0}^{I} \frac{2}{1+\delta_{M0}}\, \Re e(A_{IM}\, B_\alpha^{(\prime)\,IM\,\pm}(X))\,, \end{aligned} \tag{A.38}$$

where we have introduced

$$A_{IM} = i^{-\bar{\delta}_I^X} e^{iM\tilde{\phi}} d^I_{M0}(\theta_d)\,, \tag{A.39}$$

$$B_\alpha^{(\prime)\,IM\,\pm}(X) = i^{M+\bar{\delta}_I^X} \sum_{M'} \frac{1}{2}\,(1 \pm (-)^{M'+\delta_{X,B}}) i^{M'}\, d^I_{M'M}(\frac{\pi}{2})\, R_\alpha^{(\prime)\,IM'\,\pm}(X)\,. \tag{A.40}$$

Explicitly one finds

$$R_\alpha^{(\prime)\,\pm}(X) = \sum_I (-)^I P_I^d \sum_{M=0}^{I} \frac{2}{1+\delta_{M0}}\, d^I_{M0}(\theta_d) \begin{cases} \cos(M\tilde{\phi} - \bar{\delta}_I^X \frac{\pi}{2}) \Re e(B_\alpha^{(\prime)\,IM\,+}(X)) & \text{for } + \\ -\sin(M\tilde{\phi} - \bar{\delta}_I^X \frac{\pi}{2}) \Im m(B_\alpha^{(\prime)\,IM\,-}(X)) & \text{for } - \end{cases}, \tag{A.41}$$

It is now easy to show, using $(-)^{I+\delta_{X,B}+\bar{\delta}_I^X}=1$, that

$$(B_\alpha^{(\prime)\,IM\,\pm}(X))^* = \pm B_\alpha^{(\prime)\,IM\,\pm}(X)\,, \tag{A.42}$$

which yields

$$R_\alpha^{(\prime)\,\pm}(X) = \sum_{I=0}^{2}(-)^I P_I^d \sum_{M=0}^{I} \frac{2}{1+\delta_{M0}}\, d^I_{M0}(\theta_d)\, B_\alpha^{(\prime)\,IM\,\pm}(X) \begin{cases} \cos(M\tilde{\phi}-\bar{\delta}_I^X\frac{\pi}{2}) & \text{for } + \\ i\sin(M\tilde{\phi}-\bar{\delta}_I^X\frac{\pi}{2}) & \text{for } - \end{cases}. \tag{A.43}$$

Comparing this expression with (A.32) in conjunction with (A.2), we finally get the desired relation

$$f_\alpha^{(\prime)\,IM\,\pm}(X) = (-)^I i^{(1\mp1)/2+M+\bar{\delta}_I^X}\, \frac{2\bar{c}s_\alpha^{(\prime)\,\pm}}{1+\delta_{M0}} \sum_{M'} \frac{1}{2}\,(1\pm(-)^{M'+\delta_{X,B}})i^{M'}\, d^I_{M'M}(\frac{\pi}{2})\, R_\alpha^{(\prime)\,IM'\,\pm}(X)\,. \tag{A.44}$$

The inverse reads

$$R_\alpha^{(\prime)\,IM\,\pm}(X) = (-)^{I+M/2} i^{-(1\mp1)/2-\bar{\delta}_I^X}\, \frac{s_\alpha^{(\prime)\,\pm}}{2\bar{c}}\,(1\pm(-)^{M+\delta_{X,B}}) \sum_{M'} \frac{1}{2}\,(1+\delta_{M'0})i^{M'}\, d^I_{M'M}(\frac{\pi}{2})\, f_\alpha^{(\prime)\,IM'\,\pm}(X)\,. \tag{A.45}$$

APPENDIX B: QUADRATIC RELATIONS BETWEEN OBSERVABLES

In this appendix we will show that for a set of n independent t-matrix elements $\{t_j;\, j=1\ldots n\}$ one finds exactly $(n-1)^2$ quadratic relations between observables by which the n^2 linearly independent observables are reduced to a set of $2n-1$ independent ones. To this end we introduce the bilinear forms

$$T_{j'j} := t^*_{j'} t_j\,, \tag{B.1}$$

which can be expressed as a linear form of the observables $\mathcal{O}^\alpha$.

$$T_{j'j} = \sum_\alpha \tau^\alpha_{j'j}\,\mathcal{O}^\alpha\,, \tag{B.2}$$

with appropriate coefficients $\tau^\alpha_{j'j}$. They have the property

$$\tau^\alpha_{j'j} = \tau^{\alpha\,*}_{jj'}\,, \tag{B.3}$$

which follows from $T_{j'j}=T^*_{jj'}$ and the fact that the observables are real quantities. It is straightforward to show that these bilinear forms obey the relation

$$T_{j'j}T_{lm} = T_{j'm}T_{lj}\,, \tag{B.4}$$

which, expressed in terms of observables, yields quadratic relations between the latter. In particular, choosing $k=l=m$, one finds

$$T_{j'j} = \frac{T_{j'k}T_{kj}}{T_{kk}}\,, \tag{B.5}$$

where k can be chosen arbitrarily. It is also clear that from (B.5) one can recover the relation (B.4). Thus we only need to consider the latter relation, and the question is, how many independent quadratic relations one can find.

We first note, it is sufficient to consider only one specific k, because from (B.5) one can derive straightforwardly the analogous relation for any other k'. Second, it is sufficient to consider only the cases $j'\le j$, because $T_{jj'}=T^*_{j'j}$. The remaining relations certainly are independent because of the independency of the t-matrix elements. Choosing then first $j'=j$, the case $j'=k$ yields the identity, whereas for $j'\neq k$ one finds

$$T_{j'j'}T_{kk} = |T_{j'k}|^2\,, \tag{B.6}$$

which constitute $(n-1)$ real quadratic relations

$$\sum_{\alpha\alpha'} \tau^{\alpha}_{j'j'}\, \tau^{\alpha'}_{kk}\, \mathcal{O}^{\alpha}\, \mathcal{O}^{\alpha'} = \sum_{\alpha\alpha'} \tau^{\alpha\,*}_{j'j}\, \tau^{\alpha'}_{j'j}\, \mathcal{O}^{\alpha}\, \mathcal{O}^{\alpha'}\,. \tag{B.7}$$

As next we consider the case $i < j$ for which one has $N = n(n-1)/2$ different pairs. Again on can discard the cases $j' = k$ or $j = k$, because they do not result in quadratic relations, thus ruling out $n-1$ relations. Therefore one finds in this case ($j' < j$) a total number of

$$N - (n-1) = \frac{1}{2}(n-1)(n-2) \tag{B.8}$$

different complex quadratic relations

$$\sum_{\alpha\alpha'} \tau^{\alpha}_{j'j}\, \tau^{\alpha'}_{kk}\, \mathcal{O}^{\alpha}\, \mathcal{O}^{\alpha'} = \sum_{\alpha\alpha'} \tau^{\alpha}_{j'k}\, \tau^{\alpha'}_{kj}\, \mathcal{O}^{\alpha}\, \mathcal{O}^{\alpha'}\,. \tag{B.9}$$

Separating these into real and imaginary parts, one finds as total number of independent real quadratic relations between observables

$$(n-1) + 2\frac{1}{2}(n-1)(n-2) = (n-1)^2\,, \tag{B.10}$$

which is just the required number of relations in order to reduce the number of linearly independent observables to $n^2 - (n-1)^2 = 2n-1$ independent ones.

APPENDIX C: EXPLICIT EXPRESSIONS FOR THE MATRIX REPRESENTATION OF $\mathcal{U}^{\lambda'\lambda IM}_{\tau'\nu'\tau\nu}$

Here we list the explicit forms of the $C^{m'_1 m'_2 \lambda'_d}_{m_1 m_2 \lambda_d}(\tau'\nu'\tau\nu IM)$ of (34) for the helicity, hybrid and standard bases.

(i) For the helicity basis with labeling $(\lambda_p^{(\prime)}, \lambda_n^{(\prime)}, \lambda^{(\prime)}, \lambda_d^{(\prime)})$ one finds

$$C^{\lambda'_p \lambda'_n \lambda'_d}_{\lambda_p \lambda_n \lambda_d}(\tau'\nu'\tau\nu IM) = 2\sqrt{3}(-)^{\lambda'_p + \lambda'_n - \lambda_d + \tau' + \tau}\, \hat{\tau}'\hat{\tau}\hat{I} \begin{pmatrix} 1 & 1 & I \\ \lambda'_d & -\lambda_d & M \end{pmatrix} \begin{pmatrix} \frac{1}{2} & \frac{1}{2} & \tau' \\ \lambda'_p & -\lambda_p & \nu' \end{pmatrix} \begin{pmatrix} \frac{1}{2} & \frac{1}{2} & \tau \\ \lambda'_n & -\lambda_n & \nu \end{pmatrix}. \tag{C.1}$$

(ii) Analogously one finds in the hybrid basis with the labeling $(\tilde{\lambda}_p^{(\prime)}, \tilde{\lambda}_n^{(\prime)}, \lambda^{(\prime)}, \tilde{\lambda}_d^{(\prime)})$, where for proton, neutron and deuteron the spin projections refer to the transverse y-axis,

$$C^{\tilde{\lambda}'_p \tilde{\lambda}'_n \tilde{\lambda}'_d}_{\tilde{\lambda}_p \tilde{\lambda}_n \tilde{\lambda}_d}(\tau'\nu'\tau\nu IM) = 2\sqrt{3}\omega^{IM}_{1\tilde{\lambda}_d \tilde{\lambda}'_d} \left(\omega^{\tau'\nu'}_{\frac{1}{2}\tilde{\lambda}'_p \tilde{\lambda}_p}\right)^* \left(\omega^{\tau\nu}_{\frac{1}{2}\tilde{\lambda}'_n \tilde{\lambda}_n}\right)^*, \tag{C.2}$$

where

$$\begin{aligned} \omega^{JM}_{jm'm} &= \Omega^{JM}_{jm'jm}(\frac{\pi}{2}, -\frac{\pi}{2}, -\frac{\pi}{2}) \\ &= (-)^{j-m'}\hat{J} \sum_{M'} \begin{pmatrix} j & J & j \\ -m' & M' & m \end{pmatrix} i^{M'-M} d^J_{M'M}(\frac{\pi}{2})\,. \end{aligned} \tag{C.3}$$

(iii) Finally in the standard basis with index labeling $(s^{(\prime)}, m_s^{(\prime)}, \lambda^{(\prime)}, m_d^{(\prime)})$ one has

$$\begin{aligned} C^{s' m'_s \lambda'_d}_{s m_s \lambda_d}(\tau'\nu'\tau\nu IM) = 2\sqrt{3}(-)^{1-m_d+s'-m'_s+\tau'+\tau}\, \hat{s}\hat{s}'\hat{\tau}'\hat{\tau} \begin{pmatrix} 1 & 1 & 1 \\ m'_d & -m_d & M \end{pmatrix} \\ \sum_{S\sigma} \hat{s}^2 \begin{pmatrix} \tau' & \tau & S \\ \nu' & \nu & -\sigma \end{pmatrix} \begin{pmatrix} s' & s & S \\ m'_s & -m_s & -\sigma \end{pmatrix} \begin{Bmatrix} \frac{1}{2} & \frac{1}{2} & \tau' \\ \frac{1}{2} & \frac{1}{2} & \tau \\ s' & s & S \end{Bmatrix}. \end{aligned} \tag{C.4}$$

APPENDIX D: RELATIVE BOUNDS FOR STRUCTURE FUNCTIONS

In this section we will derive relative bounds for the various structure functions $f_\alpha^{(\prime)IM\pm}(X)$ which are based on the following theorem. Given n t-matrix elements $\{t_j;\, j=1,\ldots,n\}$ and a hermitean matrix Ω_{ij} with eigenvalues $\{\lambda_j;\, j=1,\ldots,n\}$, then the following relation holds

$$\lambda_{min} \leq \frac{tr(t^\dagger \Omega t)}{tr(t^\dagger t)} \leq \lambda_{max}\,, \tag{D.1}$$

where

$$\lambda_{min/max} = Min/Max\{\lambda_j;\, j=1,\ldots,n\}\,. \tag{D.2}$$

As we have shown in Sect. III, a general structure function can be written in the form (see (53))

$$f_\alpha^{(\prime)IM\pm}(X) = \sum_{j'j} t_{j'}^*\, \widetilde{F}_{j'j}^{(\prime)IM\pm,\,\alpha}(X)\, t_j\,, \tag{D.3}$$

where $\widetilde{F}_{j'j}^{(\prime)IM\pm,\,\alpha}(X)$ is a hermitean matrix whose explicit form is listed in Sect. III. Denoting by $\lambda_{\alpha,min/max}^{(\prime)IM\pm}(X)$ the minimal respectively maximal eigenvalue of $\widetilde{F}_{j'j}^{(\prime)IM\pm,\,\alpha}(X)$, one finds the following relative bounds.

(i) Longitudinal structure functions:

$$\frac{1}{2}\,\lambda_{L,\,min}^{IM\pm}(X) \leq \frac{f_L^{IM\pm}(X)}{f_L^{00}} \leq \frac{1}{2}\,\lambda_{L,\,max}^{IM\pm}(X)\,, \tag{D.4}$$

because

$$f_L^{00} = 2\sum_{j=1}^{6} t_j^* t_j\,. \tag{D.5}$$

(ii) Transverse and transverse-transverse interference structure functions ($\alpha = T$ and TT):

$$\frac{1}{2}\,\lambda_{\alpha,\,min}^{(\prime)IM\pm}(X) \leq \frac{f_\alpha^{(\prime)IM\pm}(X)}{f_T^{00}} \leq \frac{1}{2}\,\lambda_{\alpha,\,max}^{(\prime)IM\pm}(X)\,, \tag{D.6}$$

because

$$f_T^{00} = 2\sum_{j=7}^{18} t_j^* t_j\,. \tag{D.7}$$

(iii) Longitudinal-transverse interference structure functions:

$$\frac{1}{2}\,\lambda_{LT,\,min}^{(\prime)IM\pm}(X) \leq \frac{f_{LT}^{(\prime)IM\pm}(X)}{f_L^{00}+f_T^{00}} \leq \frac{1}{2}\,\lambda_{LT,\,max}^{(\prime)IM\pm}(X)\,, \tag{D.8}$$

because

$$f_L^{00} + f_T^{00} = 2\sum_{j=1}^{18} t_j^* t_j\,. \tag{D.9}$$

The resulting relative bounds for the various structure functions are listed in the following tables.

APPENDIX E: EXPLICIT BILINEAR EXPRESSIONS

In this appendix we will first consider one specific example of the longitudinal matrix elements using a rotated helicity basis, namely the case where only the final state spin states are rotated into the y-axis. In this case the longitudinal t-matrix elements possess the symmetry

$$t^{R_y R_0}_{\lambda_p \lambda_n 0 -\lambda_d} = (-)^{1+\lambda_p+\lambda_n+\lambda_d} t^{R_y R_0}_{\lambda_p \lambda_n 0 \lambda_d} \,. \tag{E.1}$$

The labeling of the independent matrix elements are given in Table IX. One finds the following bilinear expressions where we use the notation $f^{IM}_{L,X}$ instead of $f^{IM}_L(X)$

$$\begin{aligned}
T_{1,1} &= t^*_{\frac{1}{2}\frac{1}{2}00} t_{\frac{1}{2}\frac{1}{2}00} = \frac{1}{6}\Big(f^{00}_L - \sqrt{2}\, f^{20}_L + f^{00}_{L,\,y_1} - \sqrt{2}\, f^{20}_{L,\,y_1} \Big) \,, \\
T_{2,1} &= t^*_{-\frac{1}{2}-\frac{1}{2}00} t_{\frac{1}{2}\frac{1}{2}00} = \frac{1}{6}\Big(- f^{00}_{L,\,zz} + \sqrt{2}\, f^{20}_{L,\,zz} + i\,(f^{00}_{L,\,xz} - \sqrt{2}\, f^{20}_{L,\,xz}) \Big) \,, \\
T_{3,1} &= t^*_{\frac{1}{2}\frac{1}{2}01} t_{\frac{1}{2}\frac{1}{2}00} = \frac{1}{4\sqrt{6}}\Big(- f^{21}_L - f^{21}_{L,\,y_1} + i\,(-f^{11}_L - f^{11}_{L,\,y_1}) \Big) \,, \\
T_{4,1} &= t^*_{\frac{1}{2}-\frac{1}{2}01} t_{\frac{1}{2}\frac{1}{2}00} = \frac{1}{4\sqrt{6}}\Big(- f^{11}_{L,\,x_2} + f^{21}_{L,\,z_2} + i\,(-f^{21}_{L,\,x_2} - f^{11}_{L,\,z_2}) \Big) \,, \\
T_{5,1} &= t^*_{-\frac{1}{2}\frac{1}{2}01} t_{\frac{1}{2}\frac{1}{2}00} = \frac{1}{4\sqrt{6}}\Big(- f^{11}_{L,\,x_1} + f^{21}_{L,\,z_1} + i\,(-f^{21}_{L,\,x_1} - f^{11}_{L,\,z_1}) \Big) \,, \\
T_{6,1} &= t^*_{-\frac{1}{2}-\frac{1}{2}01} t_{\frac{1}{2}\frac{1}{2}00} = \frac{1}{4\sqrt{6}}\Big(f^{11}_{L,\,xz} + f^{21}_{L,\,zz} + i\,(-f^{21}_{L,\,xz} + f^{11}_{L,\,zz}) \Big) \,, \\
T_{2,2} &= t^*_{-\frac{1}{2}-\frac{1}{2}00} t_{-\frac{1}{2}-\frac{1}{2}00} = \frac{1}{6}\Big(f^{00}_L - \sqrt{2}\, f^{20}_L - f^{00}_{L,\,y_1} + \sqrt{2}\, f^{20}_{L,\,y_1} \Big) \,, \\
T_{3,2} &= t^*_{\frac{1}{2}\frac{1}{2}01} t_{-\frac{1}{2}-\frac{1}{2}00} = \frac{1}{4\sqrt{6}}\Big(- f^{11}_{L,\,xz} + f^{21}_{L,\,zz} + i\,(f^{21}_{L,\,xz} + f^{11}_{L,\,zz}) \Big) \,, \\
T_{4,2} &= t^*_{\frac{1}{2}-\frac{1}{2}01} t_{-\frac{1}{2}-\frac{1}{2}00} = \frac{1}{4\sqrt{6}}\Big(- f^{11}_{L,\,x_1} - f^{21}_{L,\,z_1} + i\,(-f^{21}_{L,\,x_1} + f^{11}_{L,\,z_1}) \Big) \,, \\
T_{5,2} &= t^*_{-\frac{1}{2}\frac{1}{2}01} t_{-\frac{1}{2}-\frac{1}{2}00} = \frac{1}{4\sqrt{6}}\Big(- f^{11}_{L,\,x_2} - f^{21}_{L,\,z_2} + i\,(-f^{21}_{L,\,x_2} + f^{11}_{L,\,z_2}) \Big) \,, \\
T_{6,2} &= t^*_{-\frac{1}{2}-\frac{1}{2}01} t_{-\frac{1}{2}-\frac{1}{2}00} = \frac{1}{4\sqrt{6}}\Big(- f^{21}_L + f^{21}_{L,\,y_1} + i\,(-f^{11}_L + f^{11}_{L,\,y_1}) \Big) \,, \\
T_{3,3} &= t^*_{\frac{1}{2}\frac{1}{2}01} t_{\frac{1}{2}\frac{1}{2}01} = \frac{1}{24}\Big(2\, f^{00}_L + \sqrt{2}\, f^{20}_L - \sqrt{3}\, f^{22}_L + 2\, f^{00}_{L,\,y_1} + \sqrt{2}\, f^{20}_{L,\,y_1} - \sqrt{3}\, f^{22}_{L,\,y_1} \Big) \,, \\
T_{4,3} &= t^*_{\frac{1}{2}-\frac{1}{2}01} t_{\frac{1}{2}\frac{1}{2}01} = \frac{1}{8\sqrt{3}}\Big(\sqrt{2}\, f^{10}_{L,\,x_2} + f^{22}_{L,\,z_2} + i\,(-f^{22}_{L,\,x_2} + \sqrt{2}\, f^{10}_{L,\,z_2}) \Big) \,, \\
T_{5,3} &= t^*_{-\frac{1}{2}\frac{1}{2}01} t_{\frac{1}{2}\frac{1}{2}01} = \frac{1}{8\sqrt{3}}\Big(\sqrt{2}\, f^{10}_{L,\,x_1} + f^{22}_{L,\,z_1} + i\,(-f^{22}_{L,\,x_1} + \sqrt{2}\, f^{10}_{L,\,z_1}) \Big) \,, \\
T_{6,3} &= t^*_{-\frac{1}{2}-\frac{1}{2}01} t_{\frac{1}{2}\frac{1}{2}01} = \frac{1}{24}\Big(- 2\, f^{00}_{L,\,zz} - \sqrt{2}\, f^{20}_{L,\,zz} + \sqrt{3}\, f^{22}_{L,\,zz} + i\,(2\, f^{00}_{L,\,xz} + \sqrt{2}\, f^{20}_{L,\,xz} - \sqrt{3}\, f^{22}_{L,\,xz}) \Big) \,, \\
T_{4,4} &= t^*_{\frac{1}{2}-\frac{1}{2}01} t_{\frac{1}{2}-\frac{1}{2}01} = \frac{1}{24}\Big(2\, f^{00}_L + \sqrt{2}\, f^{20}_L + \sqrt{3}\, f^{22}_L + 2\, f^{00}_{L,\,y_1} + \sqrt{2}\, f^{20}_{L,\,y_1} + \sqrt{3}\, f^{22}_{L,\,y_1} \Big) \,, \\
T_{5,4} &= t^*_{-\frac{1}{2}\frac{1}{2}01} t_{\frac{1}{2}-\frac{1}{2}01} = \frac{1}{24}\Big(2\, f^{00}_{L,\,zz} + \sqrt{2}\, f^{20}_{L,\,zz} + \sqrt{3}\, f^{22}_{L,\,zz} + i\,(-2\, f^{00}_{L,\,xz} - \sqrt{2}\, f^{20}_{L,\,xz} - \sqrt{3}\, f^{22}_{L,\,xz}) \Big) \,, \\
T_{6,4} &= t^*_{-\frac{1}{2}-\frac{1}{2}01} t_{\frac{1}{2}-\frac{1}{2}01} = \frac{1}{8\sqrt{3}}\Big(\sqrt{2}\, f^{10}_{L,\,x_1} - f^{22}_{L,\,z_1} + i\,(f^{22}_{L,\,x_1} + \sqrt{2}\, f^{10}_{L,\,z_1}) \Big) \,, \\
T_{5,5} &= t^*_{-\frac{1}{2}\frac{1}{2}01} t_{-\frac{1}{2}\frac{1}{2}01} = \frac{1}{24}\Big(2\, f^{00}_L + \sqrt{2}\, f^{20}_L + \sqrt{3}\, f^{22}_L - 2\, f^{00}_{L,\,y_1} - \sqrt{2}\, f^{20}_{L,\,y_1} - \sqrt{3}\, f^{22}_{L,\,y_1} \Big) \,, \\
T_{6,5} &= t^*_{-\frac{1}{2}-\frac{1}{2}01} t_{-\frac{1}{2}\frac{1}{2}01} = \frac{1}{8\sqrt{3}}\Big(\sqrt{2}\, f^{10}_{L,\,x_2} - f^{22}_{L,\,z_2} + i\,(f^{22}_{L,\,x_2} + \sqrt{2}\, f^{10}_{L,\,z_2}) \Big) \,, \\
T_{6,6} &= t^*_{-\frac{1}{2}-\frac{1}{2}01} t_{-\frac{1}{2}-\frac{1}{2}01} = \frac{1}{24}\Big(2\, f^{00}_L + \sqrt{2}\, f^{20}_L - \sqrt{3}\, f^{22}_L - 2\, f^{00}_{L,\,y_1} - \sqrt{2}\, f^{20}_{L,\,y_1} + \sqrt{3}\, f^{22}_{L,\,y_1} \Big) \,.
\end{aligned} \tag{E.2}$$

For obvious reasons we will choose for this case only groups of two interference terms which are represented by four observables, i.e., the six groups represented in the panels (b) through (d) in Fig. 5. Avoiding as mentioned above closed loops of three, one finds three closed loops containing four points, already shown in Fig. 5. Each of these loops can be combined with one of the remaining four groups in order to find a minimal pattern for the determination of all matrix elements by one. Thus one finds altogether twelve different combinations of three groups containing one four-loop shown diagrammatically in Fig. 6. Let us consider explicitly the case of panel (a1). It involves the group $\{T_{3,1},\, T_{6,2}\}$, $\{T_{6,1},\, T_{3,2}\}$, and $\{T_{5,3},\, T_{6,4}\}$. We will choose t_1 as real and positive and express all other matrix elements in terms of t_1 as follows (note $T_{i,j} = T^*_{j,i}$)

$$t_3 = \frac{1}{t_1}\, T_{1,3}\,, \qquad t_6 = \frac{1}{t_1}\, T_{1,6}\,, \tag{E.3}$$

$$t_2 = t_1\, \frac{T_{6,2}}{T_{6,1}}\,, \qquad t_4 = t_1\, \frac{T_{6,4}}{T_{6,1}}\,, \tag{E.4}$$

$$t_5 = t_1\, \frac{T_{3,5}}{T_{3,1}}\,. \tag{E.5}$$

Because of the closed four-loop one has from (80) the condition

$$T_{1,6} T_{2,3} = T_{2,6} T_{1,3}\,, \tag{E.6}$$

which can be used to eliminate two of the eight observables of the groups $\{T_{6,1},\, T_{3,2}\}$ and $\{T_{3,1},\, T_{6,2}\}$. Formally, there is no preference as to which observables one should eliminate. A closer inspection of the explicit expressions of the $T_{i,j}$ of each one of the three groups (see Eq. (E.2)) reveals that the general structure for the two interference terms belonging to one group is of the form

$$T_{i,j} = a_1 + a_2 + i(b_1 + b_2)\,, \qquad T_{i',j'} = a_1 - a_2 + i(b_1 - b_2)\,, \tag{E.7}$$

where a_i and b_i are observables up to some constants, and thus are real quantities. Therefore, the above relation can be written in the general form separating real and imaginary parts and denoting the observables of one group by $\{a_i, b_i\}$ and those of the other group by $\{\bar{a}_i, \bar{b}_i\}$

$$a_1^2 - a_2^2 - b_1^2 + b_2^2 = \bar{a}_1^2 - \bar{a}_2^2 - \bar{b}_1^2 + \bar{b}_2^2\,, \tag{E.8}$$

$$a_1 b_1 - a_2 b_2 = \bar{a}_1 \bar{b}_1 - \bar{a}_2 \bar{b}_2\,, \tag{E.9}$$

by which two observables can be eliminated. For example, a_1 and b_1 can be eliminated by

$$b_1 = \pm \sqrt{\frac{1}{2}(|\alpha + 2i\beta| - \alpha)}\,, \tag{E.10}$$

$$a_1 = \frac{\beta}{b_1}\,, \tag{E.11}$$

where

$$\alpha = \bar{a}_1^2 - \bar{a}_2^2 - \bar{b}_1^2 + \bar{b}_2^2 + a_2^2 - b_2^2\,, \tag{E.12}$$

$$\beta = \bar{a}_1 \bar{b}_1 - \bar{a}_2 \bar{b}_2 + a_2 b_2\,. \tag{E.13}$$

Thus all five complex matrix elements in (E.3) through (E.5) are determined by ten observables and by t_1. The latter one can be determined finally, for example, from

$$f_L = (t_1)^2 \left(1 + \left|\frac{T_{6,2}}{T_{6,1}}\right|^2 + \left|\frac{T_{6,4}}{T_{6,1}}\right|^2 + \left|\frac{T_{3,5}}{T_{3,1}}\right|^2\right) + \frac{1}{|t_1|^2}\left(|T_{1,3}|^2 + |T_{1,6}|^2\right), \tag{E.14}$$

which in general will provide two solutions.

Another possibility is to choose closed loops consisting of all six points. These are represented in Fig. 7. As an example, we will discuss the case of panel (a) containing only groups which are governed by single and double polarization observables alone. The corresponding interference terms of these groups are given by $\{T_{3,1},\, T_{6,2}\}$, $\{T_{5,1},\, T_{4,2}\}$, and $\{T_{4,3},\, T_{6,5}\}$ listed above. Again we will choose t_1 as real and positive and express all other matrix elements in terms of t_1

$$t_3 = \frac{1}{t_1}\, T_{1,3}\,, \qquad t_5 = \frac{1}{t_1}\, T_{1,5}\,, \tag{E.15}$$

$$t_4 = t_1\, \frac{T_{3,4}}{T_{3,1}}\,, \qquad t_6 = t_1\, \frac{T_{5,6}}{T_{5,1}}\,, \tag{E.16}$$

$$t_2 = \frac{1}{t_1}\, \frac{T_{1,3} T_{4,2}}{T_{4,3}}\,. \tag{E.17}$$

Furthermore, the closed loop through all six points leads to the following relation between observables

$$T_{3,4}\, T_{5,1}\, T_{2,6} = T_{5,6}\, T_{3,1}\, T_{2,4}\,. \tag{E.18}$$

It can be used to eliminate two of the twelve observables involved belonging to one group. For example, one may write

$$T_{3,4} = T_{5,6}\, T \quad \text{with} \quad T = \frac{T_{3,1}\, T_{2,4}}{T_{5,1}\, T_{2,6}}\,, \tag{E.19}$$

where $T_{3,4}$ and $T_{5,6}$ belong to one group of observables which do not appear in T.

Also here, there is no preference as to which observables one should eliminate, and again the two interference terms belonging to one group and appearing in (E.19) are of the form

$$T_{i,j} = a_1 + a_2 + i(b_1 + b_2)\,, \qquad T_{i',j'} = a_1 - a_2 - i(b_1 - b_2)\,. \tag{E.20}$$

Thus the above relation leads to

$$a_1 + a_2 + i(b_1 + b_2) = (a_1 - a_2 - i(b_1 - b_2))\, T\,, \tag{E.21}$$

where T is a ratio of the interference terms of the other two groups depending on the choice of the two interference terms $T_{i,j}$ and $T_{i',j'}$ of one group (see for example (E.19)). It is important to note that T does not depend on the observables of a_i and b_i. Then taking the real and imaginary parts of (E.21), one obtains a system of linear equations between the a_i and b_i

$$a_1 + a_2 = \Re e(T)\,(a_1 - a_2) + \Im m(T)\,(b_1 - b_2)\,, \tag{E.22}$$

$$b_1 + b_2 = \Im m(T)\,(a_1 - a_2) - \Re e(T)\,(b_1 - b_2)\,, \tag{E.23}$$

which can be used to eliminate two of the four observables. For example, if one wants to eliminate a_i, one easily finds

$$a_1 - a_2 = \frac{1}{\Im m(T)}(b_1 + b_2 + \Re e(T)\,(b_1 - b_2))\,, \tag{E.24}$$

$$a_1 + a_2 = \frac{1}{\Im m(T)}(\Re e(T)\,(b_1 + b_2) + |T|^2(b_1 - b_2))\,, \tag{E.25}$$

provided $\Im m(T) \neq 0$. The corresponding solution for b_i is obtained from this by exchanging $a_i \leftrightarrow b_i$ and changing the sign of $\Im m(T)$. If one wants to eliminate a_1 and b_1 one obtains

$$a_1 = \frac{1}{|T|^2 - 1}\Big(|1 + T|^2\, a_2 + 2\Im m(T)\, b_2\Big)\,, \tag{E.26}$$

$$b_1 = \frac{1}{|T|^2 - 1}\Big(2\Im m(T)\, a_2 + |1 + T|^2\, b_2\Big) \tag{E.27}$$

provided $|T|^2 \neq 1$. Thus all five complex matrix elements in (E.15) through (E.17) are determined by ten observables and by t_1, while the latter one can be determined, for example, as above from

$$f_L = (t_1)^2 \left(1 + \left|\frac{T_{3,4}}{T_{3,1}}\right|^2 + \left|\frac{T_{5,6}}{T_{5,1}}\right|^2\right) + \frac{1}{|t_1|^2}\left(|T_{1,3}|^2 + |T_{1,5}|^2 + \left|\frac{T_{1,3} T_{4,2}}{T_{4,3}}\right|^2\right), \tag{E.28}$$

with again two solutions in general.

Next we will consider the more involved transverse matrix elements. In this case the rotation of the spin quantization axis for the initial and/or final state does not lead to a simpler grouping of observables than shown in Fig. 8. Thus we will use the helicity basis in the following discussion. But the results apply as well to the transformed helicity

basis discussed before for the longitudinal case, although for different groups of observables. A closer inspection of the various types of groups shows that in order to obtain a diagrammatic pattern in which each point is connected to the others, not necessarily directly, one needs a proper combination of all three types of groups as distinguished in Fig. 8 by the different line types. Only the group represented by dashed lines in panel (a) of Fig. 8 has to be excluded, because it always leads with the solid-line groups to triangular loops. Thus the possible combinations of all four solid-line groups (panels (a) through (d)) with all three dashed-line and three dash-dot-dot-line groups (panels (b) through (d)) amount to 36 different patterns.

However those combinations where dashed lines run parallel to dash-dot-dot lines also have to be excluded, because they result in patterns with two disconnected groups of points. Three such combinations appear in the panels (b) through (d) of Fig. 8. Therefore, 12 of the 36 patterns have to be excluded, leaving 24 connected patterns, which can be used for the determination of all transverse t-matrix elements in terms of one. We show in Fig. 9 for the solid-line group of panel (a) in Fig. 8 the resulting six connected diagrams of which we will choose the one in panel (a) for a closer analysis. All 24 connected patterns are governed by 36 observables (16 for the solid-line groups, 12 for the dash-dot-dot ones, and 8 for the dashed ones, see Table XVI). As we will soon see, one finds six independent four-point-loops and one independent six-point-loop, through which one can eliminate 14 observables, thus resulting in 22 observables, which is just the minimal number required to express all matrix elements in terms of one.

Now we will turn to a detailed discussion of the pattern in panel (a) of Fig. 9. The diagram consists of the following groups of observables listed in Table XVI: solid lines of panel (a), dashed lines of panel (b), and dash-dot-dot lines of panel (d). The explicit bilinear expressions for the solid-line group are

$$
\begin{aligned}
T_{11,7} &= t^*_{\frac{1}{2}\frac{1}{2}11} t_{\frac{1}{2}\frac{1}{2}10} \\
&= \frac{1}{16\sqrt{6}} \Big(- f_T^{21} + f_T'^{11} - f_{T,zz}^{21} + f_{T,zz}'^{11} - f_{T,z_1}^{11} + f_{T,z_1}'^{21} - f_{T,z_2}^{11} + f_{T,z_2}'^{21} \\
&\quad + i \left(- f_T^{11} - f_T'^{21} - f_{T,zz}^{11} - f_{T,zz}'^{21} - f_{T,z_1}^{21} - f_{T,z_1}'^{11} - f_{T,z_2}^{21} - f_{T,z_2}'^{11} \right) \Big) , \\
T_{15,7} &= t^*_{\frac{1}{2}\frac{1}{2}1-1} t_{\frac{1}{2}\frac{1}{2}10} \\
&= \frac{1}{16\sqrt{6}} \Big(f_T^{21} + f_T'^{11} + f_{T,zz}^{21} + f_{T,zz}'^{11} - f_{T,z_1}^{11} - f_{T,z_1}'^{21} - f_{T,z_2}^{11} - f_{T,z_2}'^{21} \\
&\quad + i \left(f_T^{11} - f_T'^{21} + f_{T,zz}^{11} - f_{T,zz}'^{21} - f_{T,z_1}^{21} + f_{T,z_1}'^{11} - f_{T,z_2}^{21} + f_{T,z_2}'^{11} \right) \Big) , \\
T_{12,8} &= t^*_{\frac{1}{2}-\frac{1}{2}11} t_{\frac{1}{2}-\frac{1}{2}10} \\
&= \frac{1}{16\sqrt{6}} \Big(- f_T^{21} + f_T'^{11} + f_{T,zz}^{21} - f_{T,zz}'^{11} - f_{T,z_1}^{11} + f_{T,z_1}'^{21} + f_{T,z_2}^{11} - f_{T,z_2}'^{21} \\
&\quad + i \left(- f_T^{11} - f_T'^{21} + f_{T,zz}^{11} + f_{T,zz}'^{21} - f_{T,z_1}^{21} - f_{T,z_1}'^{11} + f_{T,z_2}^{21} + f_{T,z_2}'^{11} \right) \Big) , \\
T_{16,8} &= t^*_{\frac{1}{2}-\frac{1}{2}1-1} t_{\frac{1}{2}-\frac{1}{2}10} \\
&= \frac{1}{16\sqrt{6}} \Big(f_T^{21} + f_T'^{11} - f_{T,zz}^{21} - f_{T,zz}'^{11} - f_{T,z_1}^{11} - f_{T,z_1}'^{21} + f_{T,z_2}^{11} + f_{T,z_2}'^{21} \\
&\quad + i \left(f_T^{11} - f_T'^{21} - f_{T,zz}^{11} + f_{T,zz}'^{21} - f_{T,z_1}^{21} + f_{T,z_1}'^{11} + f_{T,z_2}^{21} - f_{T,z_2}'^{11} \right) \Big) , \\
T_{13,9} &= t^*_{-\frac{1}{2}\frac{1}{2}11} t_{-\frac{1}{2}\frac{1}{2}10} \\
&= \frac{1}{16\sqrt{6}} \Big(- f_T^{21} + f_T'^{11} + f_{T,zz}^{21} - f_{T,zz}'^{11} + f_{T,z_1}^{11} - f_{T,z_1}'^{21} - f_{T,z_2}^{11} + f_{T,z_2}'^{21} \\
&\quad + i \left(- f_T^{11} - f_T'^{21} + f_{T,zz}^{11} + f_{T,zz}'^{21} + f_{T,z_1}^{21} + f_{T,z_1}'^{11} - f_{T,z_2}^{21} - f_{T,z_2}'^{11} \right) \Big) , \\
T_{17,9} &= t^*_{-\frac{1}{2}\frac{1}{2}1-1} t_{-\frac{1}{2}\frac{1}{2}10} \\
&= \frac{1}{16\sqrt{6}} \Big(f_T^{21} + f_T'^{11} - f_{T,zz}^{21} - f_{T,zz}'^{11} + f_{T,z_1}^{11} + f_{T,z_1}'^{21} - f_{T,z_2}^{11} - f_{T,z_2}'^{21} \\
&\quad + i \left(f_T^{11} - f_T'^{21} - f_{T,zz}^{11} + f_{T,zz}'^{21} + f_{T,z_1}^{21} - f_{T,z_1}'^{11} - f_{T,z_2}^{21} + f_{T,z_2}'^{11} \right) \Big) , \\
T_{14,10} &= t^*_{-\frac{1}{2}-\frac{1}{2}11} t_{-\frac{1}{2}-\frac{1}{2}10} \\
&= \frac{1}{16\sqrt{6}} \Big(- f_T^{21} + f_T'^{11} - f_{T,zz}^{21} + f_{T,zz}'^{11} + f_{T,z_1}^{11} - f_{T,z_1}'^{21} + f_{T,z_2}^{11} - f_{T,z_2}'^{21}
\end{aligned}
$$

$$
\begin{aligned}
&\quad +i\,\left(-f_T^{11}-f_T'^{21}-f_{T,\,zz}^{11}-f_{T,\,zz}'^{21}+f_{T,\,z_1}^{21}+f_{T,\,z_1}'^{11}+f_{T,\,z_2}^{21}+f_{T,\,z_2}'^{11}\right)\Big)\,,\\
T_{18,10} &= t^*_{-\frac12-\frac12 1-1}t_{-\frac12-\frac12 10}\\
&= \frac{1}{16\sqrt{6}}\Big(f_T^{21}+f_T'^{11}+f_{T,\,zz}^{21}+f_{T,\,zz}'^{11}+f_{T,\,z_1}^{11}+f_{T,\,z_1}'^{21}+f_{T,\,z_2}^{11}+f_{T,\,z_2}'^{21}\\
&\quad +i\,\left(f_T^{11}-f_T'^{21}+f_{T,\,zz}^{11}-f_{T,\,zz}'^{21}+f_{T,\,z_1}^{21}-f_{T,\,z_1}'^{11}+f_{T,\,z_2}^{21}-f_{T,\,z_2}'^{11}\right)\Big)\,,
\end{aligned}
$$

for the dashed-line group

$$
\begin{aligned}
T_{16,11} &= t^*_{\frac12-\frac12 1-1}t_{\frac12\frac12 11}\\
&= \frac{1}{16\sqrt{3}}\Big(-f_{T,\,x_2}'^{22}-f_{T,\,y_2}'^{22}+f_{T,\,zx}^{22}-f_{T,\,zy}^{22}+i\,\left(-f_{T,\,x_2}^{22}-f_{T,\,y_2}^{22}-f_{T,\,zx}'^{22}+f_{T,\,zy}'^{22}\right)\Big)\,,\\
T_{15,12} &= t^*_{\frac12\frac12 1-1}t_{\frac12-\frac12 11}\\
&= \frac{1}{16\sqrt{3}}\Big(-f_{T,\,x_2}'^{22}+f_{T,\,y_2}'^{22}+f_{T,\,zx}^{22}+f_{T,\,zy}^{22}+i\,\left(-f_{T,\,x_2}^{22}+f_{T,\,y_2}^{22}-f_{T,\,zx}'^{22}-f_{T,\,zy}'^{22}\right)\Big)\,,\\
T_{18,13} &= t^*_{-\frac12-\frac12 1-1}t_{-\frac12\frac12 11}\\
&= \frac{1}{16\sqrt{3}}\Big(-f_{T,\,x_2}'^{22}-f_{T,\,y_2}'^{22}-f_{T,\,zx}^{22}+f_{T,\,zy}^{22}+i\,\left(-f_{T,\,x_2}^{22}-f_{T,\,y_2}^{22}+f_{T,\,zx}'^{22}-f_{T,\,zy}'^{22}\right)\Big)\,,\\
T_{17,14} &= t^*_{-\frac12\frac12 1-1}t_{-\frac12-\frac12 11}\\
&= \frac{1}{16\sqrt{3}}\Big(-f_{T,\,x_2}'^{22}+f_{T,\,y_2}'^{22}-f_{T,\,zx}^{22}-f_{T,\,zy}^{22}+i\,\left(-f_{T,\,x_2}^{22}+f_{T,\,y_2}^{22}+f_{T,\,zx}'^{22}+f_{T,\,zy}'^{22}\right)\Big)\,,
\end{aligned}
$$

and for the dash-dot-dot-line group

$$
\begin{aligned}
T_{9,7} &= t^*_{-\frac12\frac12 10}t_{\frac12\frac12 10}\\
&= \frac{1}{24}\Big(f_{T,\,xz}^{00}-\sqrt{2}\,f_{T,\,xz}^{20}-f_{T,\,x_1}'^{00}+\sqrt{2}\,f_{T,\,x_1}'^{20}+i\,\left(f_{T,\,yz}'^{00}-\sqrt{2}\,f_{T,\,yz}'^{20}-f_{T,\,y_1}^{00}+\sqrt{2}\,f_{T,\,y_1}^{20}\right)\Big)\,,\\
T_{10,8} &= t^*_{-\frac12-\frac12 10}t_{\frac12-\frac12 10}\\
&= \frac{1}{24}\Big(-f_{T,\,xz}^{00}+\sqrt{2}\,f_{T,\,xz}^{20}-f_{T,\,x_1}'^{00}+\sqrt{2}\,f_{T,\,x_1}'^{20}+i\,\left(-f_{T,\,yz}'^{00}+\sqrt{2}\,f_{T,\,yz}'^{20}-f_{T,\,y_1}^{00}+\sqrt{2}\,f_{T,\,y_1}^{20}\right)\Big)\,,\\
T_{13,11} &= t^*_{-\frac12\frac12 11}t_{\frac12\frac12 11}\\
&= \frac{1}{24\sqrt{2}}\Big(\sqrt{2}\,f_{T,\,xz}^{00}+f_{T,\,xz}^{20}-\sqrt{3}\,f_{T,\,xz}'^{10}+\sqrt{3}\,f_{T,\,x_1}^{10}-\sqrt{2}\,f_{T,\,x_1}'^{00}-f_{T,\,x_1}'^{20}\\
&\quad +i\,\left(-\sqrt{3}\,f_{T,\,yz}^{10}+\sqrt{2}\,f_{T,\,yz}'^{00}+f_{T,\,yz}'^{20}-\sqrt{2}\,f_{T,\,y_1}^{00}-f_{T,\,y_1}^{20}+\sqrt{3}\,f_{T,\,y_1}'^{10}\right)\Big)\,,\\
T_{14,12} &= t^*_{-\frac12-\frac12 11}t_{\frac12-\frac12 11}\\
&= \frac{1}{24\sqrt{2}}\Big(-\sqrt{2}\,f_{T,\,xz}^{00}-f_{T,\,xz}^{20}+\sqrt{3}\,f_{T,\,xz}'^{10}+\sqrt{3}\,f_{T,\,x_1}^{10}-\sqrt{2}\,f_{T,\,x_1}'^{00}-f_{T,\,x_1}'^{20}\\
&\quad +i\,\left(\sqrt{3}\,f_{T,\,yz}^{10}-\sqrt{2}\,f_{T,\,yz}'^{00}-f_{T,\,yz}'^{20}-\sqrt{2}\,f_{T,\,y_1}^{00}-f_{T,\,y_1}^{20}+\sqrt{3}\,f_{T,\,y_1}'^{10}\right)\Big)\,,\\
T_{17,15} &= t^*_{-\frac12\frac12 1-1}t_{\frac12\frac12 1-1}\\
&= \frac{1}{24\sqrt{2}}\Big(\sqrt{2}\,f_{T,\,xz}^{00}+f_{T,\,xz}^{20}+\sqrt{3}\,f_{T,\,xz}'^{10}-\sqrt{3}\,f_{T,\,x_1}^{10}-\sqrt{2}\,f_{T,\,x_1}'^{00}-f_{T,\,x_1}'^{20}\\
&\quad +i\,\left(\sqrt{3}\,f_{T,\,yz}^{10}+\sqrt{2}\,f_{T,\,yz}'^{00}+f_{T,\,yz}'^{20}-\sqrt{2}\,f_{T,\,y_1}^{00}-f_{T,\,y_1}^{20}-\sqrt{3}\,f_{T,\,y_1}'^{10}\right)\Big)\,,\\
T_{18,16} &= t^*_{-\frac12-\frac12 1-1}t_{\frac12-\frac12 1-1}\\
&= \frac{1}{24\sqrt{2}}\Big(-\sqrt{2}\,f_{T,\,xz}^{00}-f_{T,\,xz}^{20}-\sqrt{3}\,f_{T,\,xz}'^{10}-\sqrt{3}\,f_{T,\,x_1}^{10}-\sqrt{2}\,f_{T,\,x_1}'^{00}-f_{T,\,x_1}'^{20}\\
&\quad +i\,\left(-\sqrt{3}\,f_{T,\,yz}^{10}-\sqrt{2}\,f_{T,\,yz}'^{00}-f_{T,\,yz}'^{20}-\sqrt{2}\,f_{T,\,y_1}^{00}-f_{T,\,y_1}^{20}-\sqrt{3}\,f_{T,\,y_1}'^{10}\right)\Big)\,.
\end{aligned}
$$

One finds six independent 4-point loops, namely (7-9-17-15), (7-9-13-11), (8-10-14-12), (8-10-18-16), (11-13-18-16), and (12-14-17-15). They all involve two dash-dot-dot-lines and lead to the following relations according to (80)

$$T_{15,17}T_{9,7} = T_{9,17}T_{15,7}\,, \quad \text{for (7-9-17-15)}\,, \tag{E.29}$$
$$T_{11,13}T_{9,7} = T_{9,13}T_{11,7}\,, \quad \text{for (7-9-13-11)}\,, \tag{E.30}$$
$$T_{12,14}T_{10,8} = T_{10,14}T_{12,8}\,, \quad \text{for (8-10-14-12)}\,, \tag{E.31}$$
$$T_{16,18}T_{10,8} = T_{10,18}T_{16,8}\,, \quad \text{for (8-10-18-16)}\,, \tag{E.32}$$
$$T_{16,18}T_{13,11} = T_{13,18}T_{16,11}\,, \quad \text{for (11-13-18-16)}\,, \tag{E.33}$$
$$T_{15,17}T_{14,12} = T_{14,17}T_{15,12}\,, \quad \text{for (12-14-17-15)}\,. \tag{E.34}$$

These relations can be used to eliminate all 12 observables of the dash-dot-dot group. Furthermore, one finds four 6-point-loops. Two of them, (7-9-13-18-16-11) and (8-10-14-17-15-12) contain two dash-dot-dot-lines and do not lead to new relations, in fact the corresponding relations can be obtained by a proper multiplication of the relations in (E.30) and (E.33), and (E.31) and (E.34), respectively. Of the other two, which involve only solid lines (4) and dashed lines (2), one is a new condition

$$T_{15,12}T_{8,16}T_{11,7} = T_{11,16}T_{8,12}T_{15,7}\,, \tag{E.35}$$

allowing to eliminate two observables of the dashed-line-group while the second one,

$$T_{14,17}T_{9,13}T_{18,10} = T_{18,13}T_{9,17}T_{14,10}\,, \tag{E.36}$$

is equivalent to the former one, because the corresponding relation is obtained from the former one by a proper multiplication of all 4-loop conditions. This then leaves the minimal number of 22 observables for describing all interference terms and only one further observable is needed to fix the last t-matrix element. However, one will find then discrete ambiguities due to the elimination of observables using the above quadratic relations. We note in passing that the result obtained for panel (a) of Fig. 9 with regard to the elimination of all observables of the dash-dot-dot-line group and two of the dashed-line group is also valid for the other five panels in Fig. 9 as well as for the corresponding connected diagrams constructed with the other solid-line groups of Fig. 8.

TABLE I. Cartesian polarization components of the outgoing nucleons and their division into the A-type and B-type observables.

X	1	y_1	y_2	xx	yy	zz	xz	zx	x_1	x_2	z_1	z_2	xy	yx	yz	zy
type	A	A	A	A	A	A	A	A	B	B	B	B	B	B	B	B

TABLE II. Transformation from cartesian to spherical polarization components of the outgoing nucleons.

α	s_α^{00}	s_α^{11}	s_α^{10}	s_α^{1-1}
0	1	0	0	0
1	0	$-1/\sqrt{2}$	0	$1/\sqrt{2}$
2	0	$i/\sqrt{2}$	0	$i/\sqrt{2}$
3	0	0	1	0

TABLE III. Nomenclature for the diagrammatic representation of groups of longitudinal observables in Fig. 2 determining the interference terms of t-matrix elements for the helicity basis, where $f_L^{IM}(X)$ is represented by X^{IM}.

Panel	Line type	Observables
(a)	solid	x_1^{10}, x_2^{22}, y_1^{00}, y_1^{20}, xz^{00}, xz^{20}
(b)	solid	1^{11}, 1^{21}, z_1^{11}, z_2^{11}, z_1^{21}, z_2^{21}, zz^{11}, zz^{21}
(c)	solid	1^{22}, z_1^{22}, z_2^{22}, zz^{22}
	dashed	x_2^{10}, x_1^{22}, y_1^{22}, xz^{22}
(d)	solid	x_1^{11}, x_2^{11}, x_1^{21}, x_2^{21}, y_1^{11}, y_1^{21}, xz^{11}, xz^{21}.

TABLE IV. Nomenclature for the diagrammatic representation of groups of longitudinal observables in Fig. 3 determining the interference terms of t-matrix elements for the hybrid basis, where $f_L^{IM}(X)$ is represented by X^{IM}.

Panel	Line type	Observables
(a)	solid	1^{20}, 1^{21}, 1^{22}, y_1^{20}, y_1^{21}, y_1^{22}
	dashed	xz^{20}, xz^{21}, xz^{22}, zz^{20}, zz^{21}, zz^{22}
(b)	solid	x_2^{10}, x_2^{11}, x_2^{21}, x_2^{22}, z_2^{10}, z_2^{11}, z_2^{21}, z_2^{22}
(c)	solid	xz^{00}, xz^{11}, xz^{20}, xz^{22}, zz^{00}, zz^{11}, zz^{20}, zz^{22}
(d)	solid	x_1^{10}, x_1^{11}, x_1^{21}, x_1^{22}, z_1^{10}, z_1^{11}, z_1^{21}, z_1^{22}

TABLE V. Nomenclature for the diagrammatic representation of groups of longitudinal observables in Fig. 4 determining the interference terms of t-matrix elements for the standard basis, where $f_L^{IM}(X)$ is represented by X^{IM}. A group in brackets with the line type as subscript indicates a subgroup determining the corresponding interference term.

Panel	Line type	Observables
(a)	solid	1^{22}, z_1^{22}, z_2^{22}, zz^{22}
	dashed	z_1^{10}, z_2^{10}, z_1^{22}, z_2^{22}
(b)	solid	x_1^{10}, x_2^{10}. x_1^{22}, x_2^{22}, $(y_1^{00}, y_1^{20}, xz^{00}, xz^{20})_{\text{dashed}}$, y_1^{22}, xz^{22}
(c)	solid	$(x_1^{11}, x_2^{11}, x_1^{21}, x_2^{21})_{\text{dashed}}$, $(y_1^{11}, y_1^{21}, xz^{11}, xz^{21})_{\text{dotted}}$
(d)	solid	$(1^{11}, 1^{21}, zz^{11}, zz^{21})_{\text{dashed}}$, $(z_1^{11}, z_2^{11}, z_1^{21}, z_2^{21})_{\text{dotted}}$

TABLE VI. Nomenclature for the diagrammatic representation of groups of longitudinal observables in Fig. 5 determining the interference terms of t-matrix elements for the transformed helicity basis, where $f_L^{IM}(X)$ is represented by X^{IM}.

Panel	Line type	Observables
(a)	solid	xz^{00}, xz^{20}, xz^{22}, zz^{00}, zz^{20}, zz^{22}
(b)	solid	1^{11}, 1^{21}, y_1^{11}, y_1^{21}
	dashed	xz^{11}, xz^{21}, zz^{11}, zz^{21}
(c)	solid	x_1^{10}, x_1^{22}, z_1^{10}, z_1^{22}
	dashed	x_2^{10}, x_2^{22}, z_2^{10}, z_2^{22}
(d)	solid	x_1^{11}, x_1^{21}, z_1^{11}, z_1^{21}
	dashed	x_2^{11}, x_2^{21}, z_2^{11}, z_2^{21}

TABLE VII. Numbering of independent longitudinal t-matrix elements ($\lambda = 0$) of $d(e, e'N)N$ for the helicity basis.

j	1	2	3	4	5	6
λ_p	$\frac{1}{2}$	$\frac{1}{2}$	$\frac{1}{2}$	$\frac{1}{2}$	$\frac{1}{2}$	$\frac{1}{2}$
λ_n	$-\frac{1}{2}$	$\frac{1}{2}$	$-\frac{1}{2}$	$\frac{1}{2}$	$-\frac{1}{2}$	$\frac{1}{2}$
λ_d	0	0	-1	-1	1	1

TABLE VIII. Numbering of independent transverse t-matrix elements ($\lambda = 1$) of $d(e, e'N)N$ for the helicity basis.

j	7	8	9	10	11	12	13	14	15	16	17	18
λ_p	$\frac{1}{2}$	$\frac{1}{2}$	$-\frac{1}{2}$	$-\frac{1}{2}$	$\frac{1}{2}$	$\frac{1}{2}$	$-\frac{1}{2}$	$-\frac{1}{2}$	$\frac{1}{2}$	$\frac{1}{2}$	$-\frac{1}{2}$	$-\frac{1}{2}$
λ_n	$\frac{1}{2}$	$-\frac{1}{2}$	$\frac{1}{2}$	$-\frac{1}{2}$	$\frac{1}{2}$	$-\frac{1}{2}$	$\frac{1}{2}$	$-\frac{1}{2}$	$\frac{1}{2}$	$-\frac{1}{2}$	$\frac{1}{2}$	$-\frac{1}{2}$
λ_d	0	0	0	0	1	1	1	1	-1	-1	-1	-1

TABLE IX. Numbering of independent longitudinal t-matrix elements ($\lambda = 0$) of $d(e, e'N)N$ for the transformed helicity basis with $R_f = R_y$ and $R_d = R_0 = R(0, 0, 0)$.

j	1	2	3	4	5	6
λ_p	$\frac{1}{2}$	$-\frac{1}{2}$	$\frac{1}{2}$	$\frac{1}{2}$	$-\frac{1}{2}$	$-\frac{1}{2}$
λ_n	$\frac{1}{2}$	$-\frac{1}{2}$	$\frac{1}{2}$	$-\frac{1}{2}$	$\frac{1}{2}$	$-\frac{1}{2}$
λ_d	0	0	1	1	1	1

TABLE X. Exact values for the real and imaginary parts of the longitudinal t-matrix elements and their average values obtained with the experimental simulation for cases A and B in units of 10 fm. The number in brackets denotes the number of check observables. Enumeration of t-matrix elements according to Table VII.

	exact	case A (1)	case A (2)	case B (1)	case B (2)
$\Re e(t_1)$	0.1360	0.1316	0.1339	0.1349	0.1364
$\Re e(t_2)$	-0.0660	-0.0681	-0.0722	-0.0660	-0.0668
$\Im m(t_2)$	0.0385	0.0308	0.0389	0.0381	0.0392
$\Re e(t_3)$	0.1285	0.1265	0.1178	0.1260	0.1266
$\Im m(t_3)$	-0.2090	-0.1918	-0.2053	-0.2067	-0.2088
$\Re e(t_4)$	-0.1620	-0.1491	-0.1631	-0.1625	-0.1622
$\Im m(t_4)$	0.0310	0.0428	0.0353	0.0314	0.0321
$\Re e(t_5)$	-0.0460	-0.0469	-0.0402	-0.0456	-0.0451
$\Im m(t_5)$	0.0338	0.0274	0.0317	0.0344	0.0342
$\Re e(t_6)$	0.1850	0.1842	0.1867	0.1834	0.1852
$\Im m(t_6)$	-0.0488	-0.0444	-0.0560	-0.0484	-0.0496

TABLE XI. Standard deviation in the experimental simulation of the longitudinal t-matrix elements from the average values of Table X in units of 10 fm, notation as in Table X.

	case A (1)	case A (2)	case B (1)	case B (2)
$\Re e(t_1)$	0.0208	0.0103	0.0119	0.0013
$\Re e(t_2)$	0.0188	0.0109	0.0066	0.0019
$\Im m(t_2)$	0.0249	0.0068	0.0108	0.0013
$\Re e(t_3)$	0.0344	0.0148	0.0145	0.0043
$\Im m(t_3)$	0.0418	0.0204	0.0242	0.0023
$\Re e(t_4)$	0.0468	0.0259	0.0161	0.0019
$\Im m(t_4)$	0.0356	0.0188	0.0216	0.0033
$\Re e(t_5)$	0.0312	0.0168	0.0138	0.0026
$\Im m(t_5)$	0.0313	0.0197	0.0073	0.0025
$\Re e(t_6)$	0.0321	0.0154	0.0201	0.0024
$\Im m(t_6)$	0.0308	0.0199	0.0166	0.0031

TABLE XII. Selected complete sets for the numerical solution of the transverse t-matrix elements.

1^{00}	1^{11}	1^{20}	1^{21}	1^{22}	$1'^{10}$	$1'^{11}$	$1'^{21}$	$1'^{22}$	y_1^{00}	y_1^{11}	y_1^{20}
	y_1^{21}	y_1^{22}	$y_1'^{10}$	$y_1'^{11}$	$y_1'^{21}$	$y_1'^{22}$	x_1^{10}	x_1^{11}	$x_1'^{00}$	$x_1'^{11}$	$x_1'^{20}$
1^{00}	1^{11}	1^{21}	$1'^{11}$	$1'^{21}$	z_1^{11}	z_1^{21}	$z_1'^{11}$	$z_1'^{21}$	x_2^{22}	$x_2'^{22}$	y_2^{22}
	$y_2'^{22}$	z_2^{11}	z_2^{21}	$z_2'^{11}$	$z_2'^{21}$	zx^{22}	zy^{22}	zz^{11}	zz^{21}	zz'^{11}	zz'^{21}

TABLE XIII. Listing of bounds for longitudinal and transverse structure functions $f_L^{IM}(X)$ and $f_T^{IM}(X)$.

I	M	$\lambda_{min}/2$	$\lambda_{max}/2$
		$X = 1$	
1	1	$-\sqrt{3}$	$\sqrt{3}$
2	0	$-\sqrt{2}$	$1/\sqrt{2}$
2	1	$-\sqrt{3}$	$\sqrt{3}$
2	2	$-\sqrt{3}$	$\sqrt{3}$
		$X = y_1,\, y_2,\, xx,\, xz,\, zx$	
0	0	-1	1
1	1	$-\sqrt{3}$	$\sqrt{3}$
2	0	$-\sqrt{2}$	$\sqrt{2}$
2	1	$-\sqrt{3}$	$\sqrt{3}$
2	2	$-\sqrt{3}$	$\sqrt{3}$
		$X = x_1,\, x_2,\, z_1,\, z_2$	
1	0	$-\sqrt{3/2}$	$\sqrt{3/2}$
1	1	$-\sqrt{3}$	$\sqrt{3}$
2	1	$-\sqrt{3}$	$\sqrt{3}$
2	2	$-\sqrt{3}$	$\sqrt{3}$

TABLE XIV. Listing of bounds for transverse and transverse interference structure functions $f_T'^{IM}(X)$ and $f_{TT}^{IM\pm}(X)$.

I	M	$\lambda_{min}/2$	$\lambda_{max}/2$
		$f_T'^{IM}(X),\, f_{TT}^{IM-}(X) : X = 1,\, y_1,\, y_2,\, xx,\, xz,\, zx;$ $f_{TT}^{IM+}(X) : X = x_1,\, x_2,\, z_1,\, z_2$	
1	0	$-\sqrt{3/2}$	$\sqrt{3/2}$
1	1	$-\sqrt{3}$	$\sqrt{3}$
2	1	$-\sqrt{3}$	$\sqrt{3}$
2	2	$-\sqrt{3}$	$\sqrt{3}$
		$f_T'^{IM}(X),\, f_{TT}^{IM-}(X) : X = x_1,\, x_2,\, z_1,\, z_2;$ $f_{TT}^{IM+}(X) : X = 1,\, y_1,\, y_2,\, xx,\, xz,\, zx$	
0	0	-1	1
1	1	$-\sqrt{3}$	$\sqrt{3}$
2	0	$-\sqrt{2}$	$\sqrt{2}$
2	1	$-\sqrt{3}$	$\sqrt{3}$
2	2	$-\sqrt{3}$	$\sqrt{3}$

TABLE XV. Listing of bounds for longitudinal-transverse interference structure functions $f_{LT}^{IM\pm}(X)$ and $f_{LT}'^{IM\pm}(X)$.

I	M	$\lambda_{min}/2$	$\lambda_{max}/2$
		$f_{LT}^{IM+}(X),\, f_{LT}'^{IM+}(X) : X = 1,\, y_1,\, y_2,\, xx,\, xz,\, zx;$ $f_{LT}^{IM-}(X),\, f_{LT}'^{IM-}(X) : X = x_1,\, x_2,\, z_1,\, z_2$	
0	0	$-\sqrt{2}$	$\sqrt{2}$
1	1	$-\sqrt{6}$	$\sqrt{6}$
2	0	-2	2
2	1	$-\sqrt{6}$	$\sqrt{6}$
2	2	$-\sqrt{6}$	$\sqrt{6}$
		$f_{LT}^{IM+}(X),\, f_{LT}'^{IM+}(X) : X = x_1,\, x_2,\, z_1,\, z_2;$ $f_{LT}^{IM-}(X),\, f_{LT}'^{IM-}(X) : X = 1,\, y_1,\, y_2,\, xx,\, xz,\, zx$	
1	0	$-\sqrt{3}$	$\sqrt{3}$
1	1	$-\sqrt{6}$	$\sqrt{6}$
2	1	$-\sqrt{6}$	$\sqrt{6}$
2	2	$-\sqrt{6}$	$\sqrt{6}$

TABLE XVI. Nomenclature for the diagrammatic representation of groups of transverse observables in Fig. 8 determining the interference terms of t-matrix elements for the helicity basis, where $f_T^{(\prime)\,IM}(X)$ is represented by $X^{(\prime)\,IM}$.

Panel	Line type	Observables
(a)	solid	1^{11}, 1^{21}, z_1^{11}, z_1^{21}, z_2^{11}, z_2^{21}, zz^{11}, zz^{21}, $1'^{11}$, $1'^{21}$, $z_1'^{11}$, $z_1'^{21}$, $z_2'^{11}$, $z_2'^{21}$, zz'^{11}, zz'^{21}
	dashed	1^{22}, z_1^{22}, z_2^{22}, zz^{22}, $1'^{22}$, $z_1'^{22}$, $z_2'^{22}$, zz'^{22}
(b)	solid	x_2^{11}, x_2^{21}, y_2^{11}, y_2^{21}, zx^{11}, zx^{21}, zy^{11}, zy^{21}, $x_2'^{11}$, $x_2'^{21}$, $y_2'^{11}$, $y_2'^{21}$, zx'^{11}, zx'^{21}, zy'^{11}, zy'^{21}
	dashed	x_2^{22}, y_2^{22}, zx^{22}, zy^{22}, $x_2'^{22}$, $y_2'^{22}$, zx'^{22}, zy'^{22}
	dash-dot-dot	x_2^{10}, y_2^{00}, y_2^{20}, zx^{00}, zx^{20}, zy^{10}, $x_2'^{00}$, $x_2'^{20}$, $y_2'^{10}$, zx'^{10}, zy'^{00}, zy'^{20}
(c)	solid	xx^{11}, xx^{21}, xy^{11}, xy^{21}, yx^{11}, yx^{21}, yy^{11}, yy^{21}, xx'^{11}, xx'^{21}, xy'^{11}, xy'^{21}, yx'^{11}, yx'^{21}, yy'^{11}, yy'^{21}
	dashed	xx^{22}, xy^{22}, yx^{22}, yy^{22}, xx'^{22}, xy'^{22}, yx'^{22}, yy'^{22}
	dash-dot-dot	xx^{00}, xx^{20}, xy^{10}, yx^{10}, yy^{00}, yy^{20}, yy'^{10}, xx'^{10}, xy'^{00}, xy'^{20}, yx'^{00}, yx'^{20}
(d)	solid	x_1^{11}, x_1^{21}, y_1^{11}, y_1^{21}, xz^{11}, xz^{21}, yz^{11}, yz^{21}, $x_1'^{11}$, $x_1'^{21}$, $y_1'^{11}$, $y_1'^{21}$, xz'^{11}, xz'^{21}, yz'^{11}, yz'^{21}
	dashed	x_1^{22}, y_1^{22}, xz^{22}, yz^{22}, $x_1'^{22}$, $y_1'^{22}$, xz'^{22}, yz'^{22}
	dash-dot-dot	x_1^{10}, y_1^{00}, y_1^{20}, xz^{00}, xz^{20}, yz^{10}, $x_1'^{00}$, $x_1'^{20}$, $y_1'^{10}$, xz'^{10}, yz'^{00}, yz'^{20}

TABLE XVII. Nomenclature for the diagrammatic representation of groups of transverse observables in Fig. 8 determining the interference terms of t-matrix elements for the transformed helicity basis, where $f_T^{(\prime)\,IM}(X)$ is represented by $X^{(\prime)\,IM}$.

Panel	Line type	Observables
(a)	solid	1^{11}, 1^{21}, y_1^{11}, y_1^{21}, y_2^{11}, y_2^{21}, yy^{11}, yy^{21}, $1'^{11}$, $1'^{21}$, $y_1'^{11}$, $y_1'^{21}$, $y_2'^{11}$, $y_2'^{21}$, yy'^{11}, yy'^{21}
	dashed	1^{22}, y_1^{22}, y_2^{22}, yy^{22}, $1'^{22}$, $y_1'^{22}$, $y_2'^{22}$, yy'^{22}
(b)	solid	x_2^{11}, x_2^{21}, z_2^{11}, z_2^{21}, yx^{11}, yx^{21}, yz^{11}, yz^{21}, $x_2'^{11}$, $x_2'^{21}$, $z_2'^{11}$, $z_2'^{21}$, yx'^{11}, yx'^{21}, yz'^{11}, yz'^{21}
	dashed	x_2^{22}, z_2^{22}, yx^{22}, yz^{22}, $x_2'^{22}$, $z_2'^{22}$, yx'^{22}, yz'^{22}
	dash-dot-dot	x_2^{10}, z_2^{10}, yx^{10}, yz^{10}, $x_2'^{00}$, $x_2'^{20}$, $z_2'^{00}$, $z_2'^{20}$, yx'^{00}, yx'^{20}, yz'^{00}, yz'^{20}
(c)	solid	xx^{11}, xx^{21}, xz^{11}, xz^{21}, zx^{11}, zx^{21}, zz^{11}, zz^{21}, xx'^{11}, xx'^{21}, xz'^{11}, xz'^{21}, zx'^{11}, zx'^{21}, zz'^{11}, zz'^{21}
	dashed	xx^{22}, xz^{22}, zx^{22}, zz^{22}, xx'^{22}, xz'^{22}, zx'^{22}, zz'^{22}
	dash-dot-dot	xx^{00}, xx^{20}, xz^{00}, xz^{20}, zx^{00}, zx^{20}, zz^{00}, zz^{20}, xx'^{10}, xz'^{10}, zx'^{10}, zz'^{10},
(d)	solid	x_1^{11}, x_1^{21}, z_1^{11}, z_1^{21}, xy^{11}, xy^{21}, zy^{11}, zy^{21}, $x_1'^{11}$, $x_1'^{21}$, $z_1'^{11}$, $z_1'^{21}$, xy'^{11}, xy'^{21}, zy'^{11}, zy'^{21},
	dashed	x_1^{22}, z_1^{22}, xy^{22}, zy^{22}, $x_1'^{22}$, $z_1'^{22}xy'^{22}$, zy'^{22}
	dash-dot-dot	x_1^{10}, z_1^{10}, xy^{10}, zy^{10}, $x_1'^{00}$, $x_1'^{20}$, $z_1'^{00}$, $z_1'^{20}$, xy'^{00}, xy'^{20}, zy'^{00}, zy'^{20}

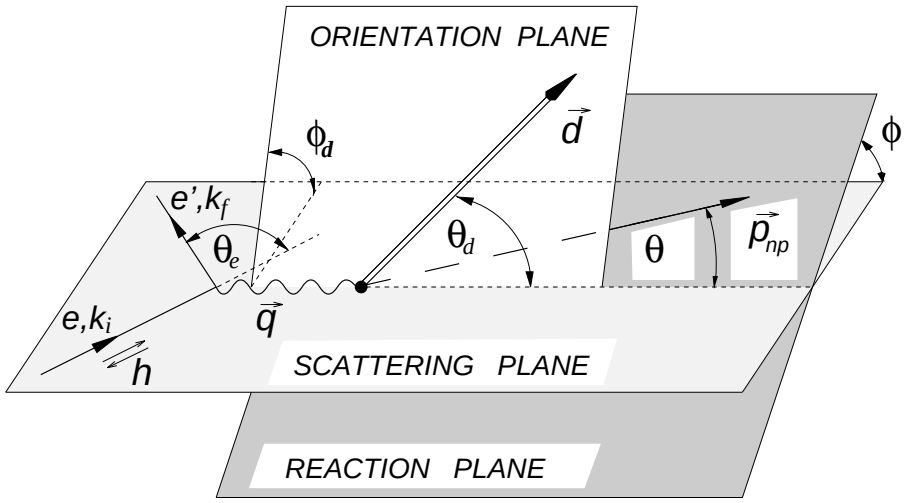

FIG. 1. Geometry of exclusive electron-deuteron scattering with polarized electrons and an oriented deuteron target. The relative np momentum, denoted by $\vec{p}_{np}$, is characterized by angles $\theta = \theta_{np}$ and $\phi = \phi_{np}$ where the deuteron orientation axis, denoted by $\vec{d}$, is specified by angles θ_d and ϕ_d.

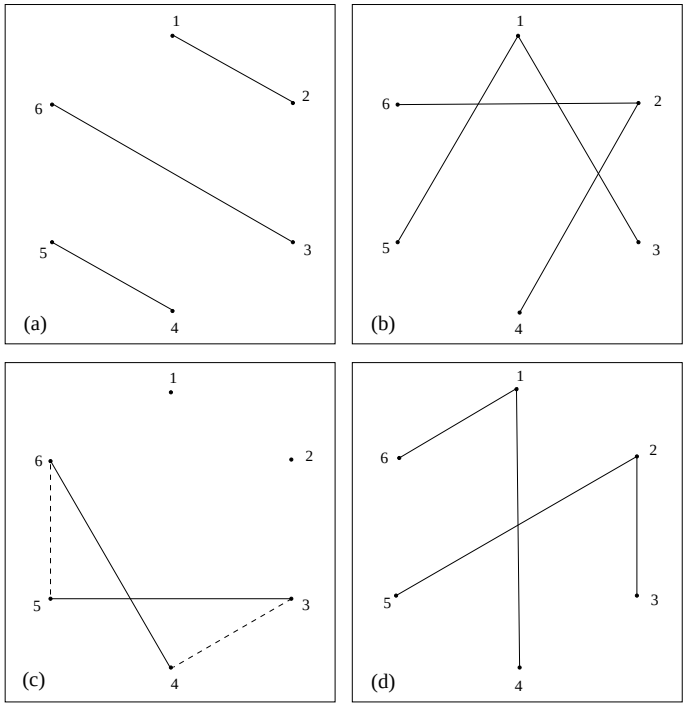

FIG. 2. Diagrammatic representation of groups of longitudinal observables determining the interference terms of t-matrix elements for the helicity basis. The nomenclature for the groups and the corresponding observables are listed in Table III.

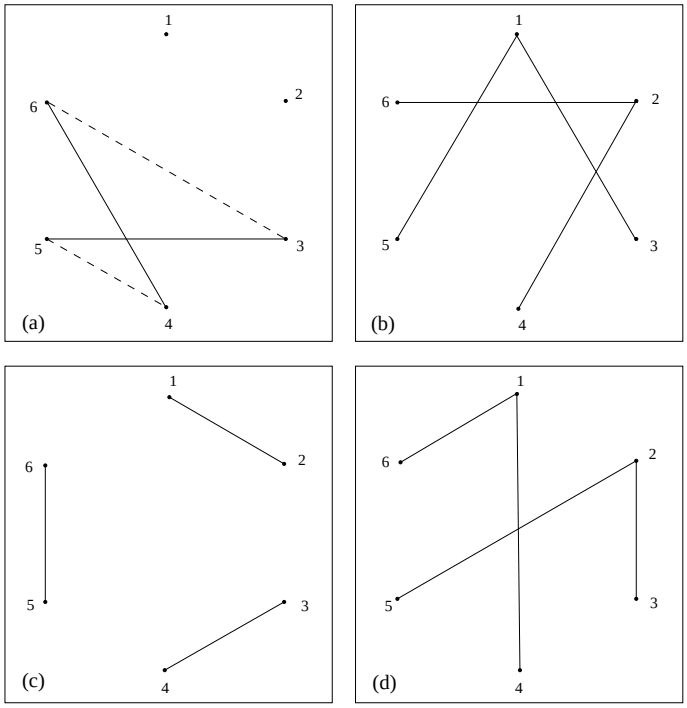

FIG. 3. As Fig. 2 for the hybrid basis with nomenclature in Table IV.

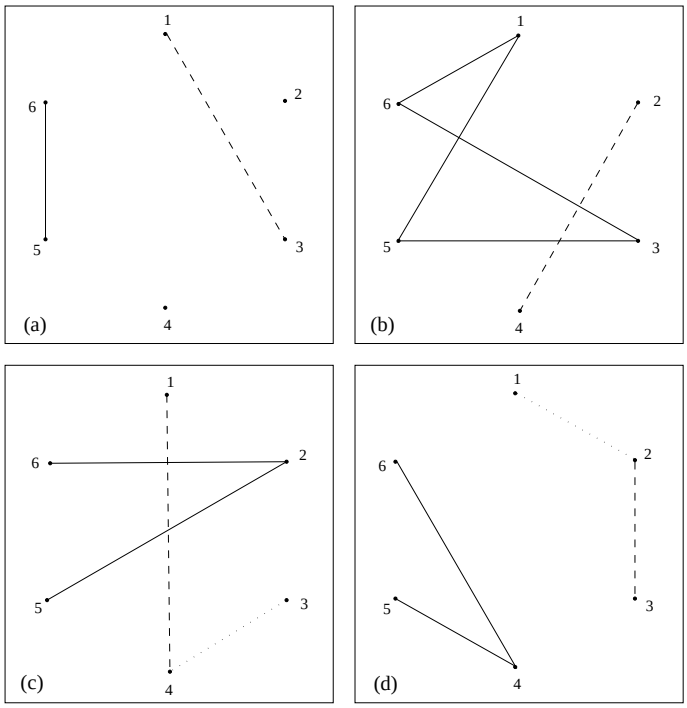

FIG. 4. As Fig. 2 for the standard basis with nomenclature in Table V.

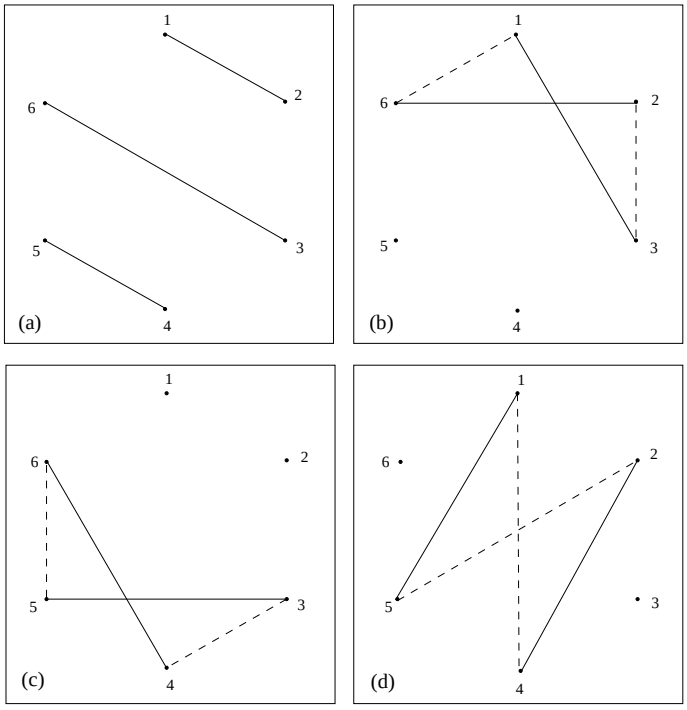

FIG. 5. As Fig. 2 for the transformed helicity basis with nomenclature in Table VI.

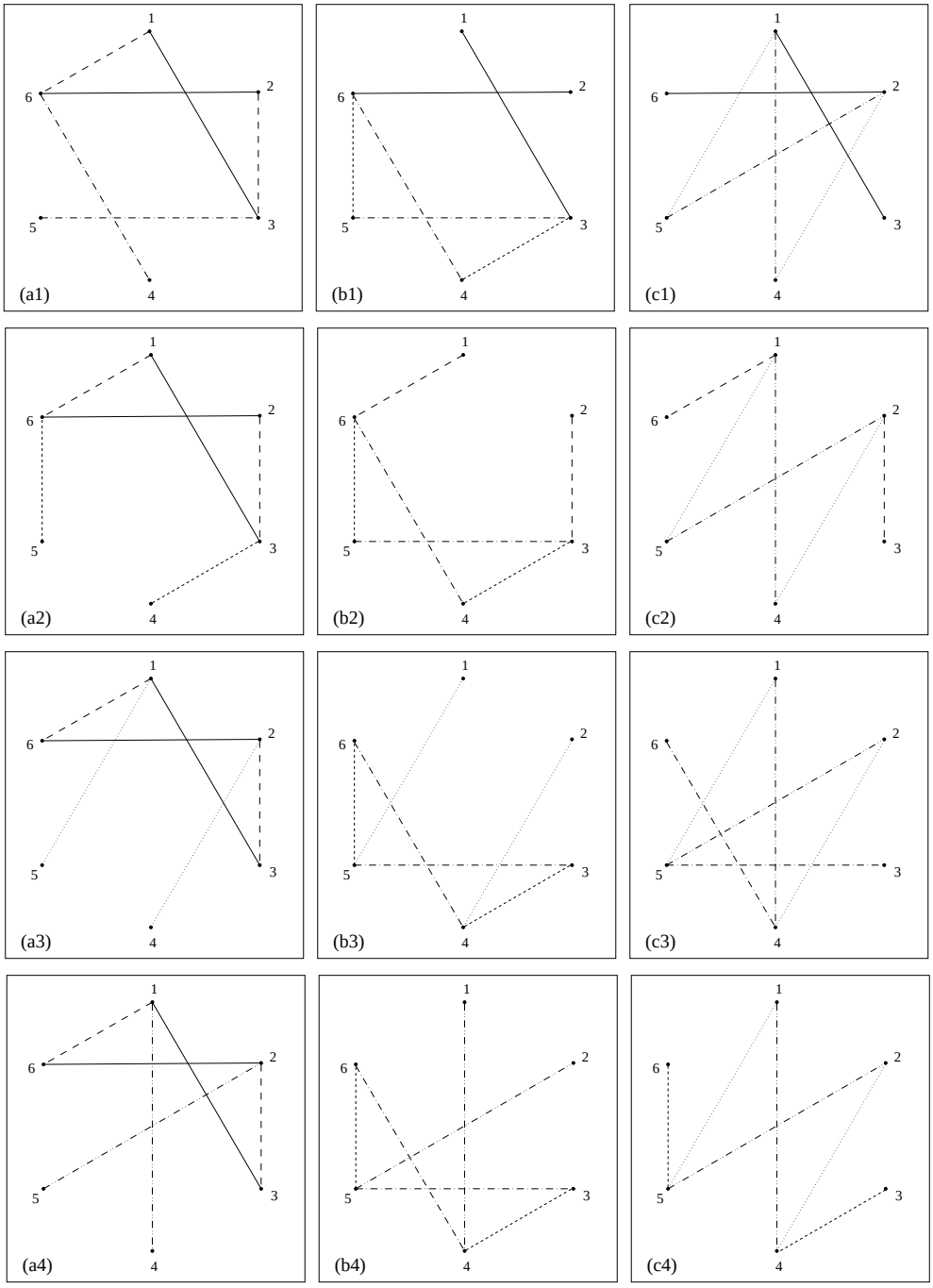

FIG. 6. Connected diagrams with three groups of longitudinal observables describing six different interference terms and containing closed loops with four points allowing a complete determination of five t-matrix elements as function of the remaining one for the transformed helicity basis where $f_L^{IM}(X)$ is represented by X^{IM}: solid: 1^{21}, 1^{11}, y_1^{11}, y_1^{21}, long dashed: xz^{11}, xz^{21}, zz^{11}, zz^{21}, dash-dotted: x_1^{10}, x_1^{22}, z_1^{10}, z_1^{22}, short dashed: x_2^{10}, x_2^{22}, z_2^{10}, z_2^{22}, dotted: x_1^{11}, x_1^{21}, z_1^{11}, z_1^{21}, dash-double-dot: x_2^{11}, x_2^{21}, z_2^{11}, z_2^{21}.

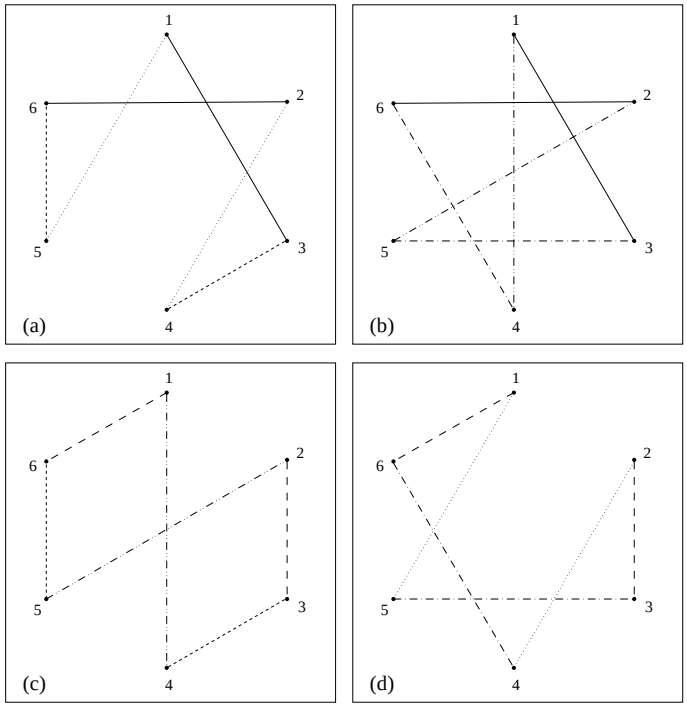

FIG. 7. As Fig. 6 containing closed loops with six points: solid: 1^{21}, 1^{11}, y_1^{11}, y_1^{21}, long dashed: xz^{11}, xz^{21}, zz^{11}, zz^{21}, dash-dotted: x_1^{10}, x_1^{22}, z_1^{10}, z_1^{22}, short dashed: x_2^{10}, x_2^{22}, z_2^{10}, z_2^{22}, dotted: x_1^{11}, x_1^{21}, z_1^{11}, z_1^{21}, dash-double-dot: x_2^{11}, x_2^{21}, z_2^{11}. z_2^{21},

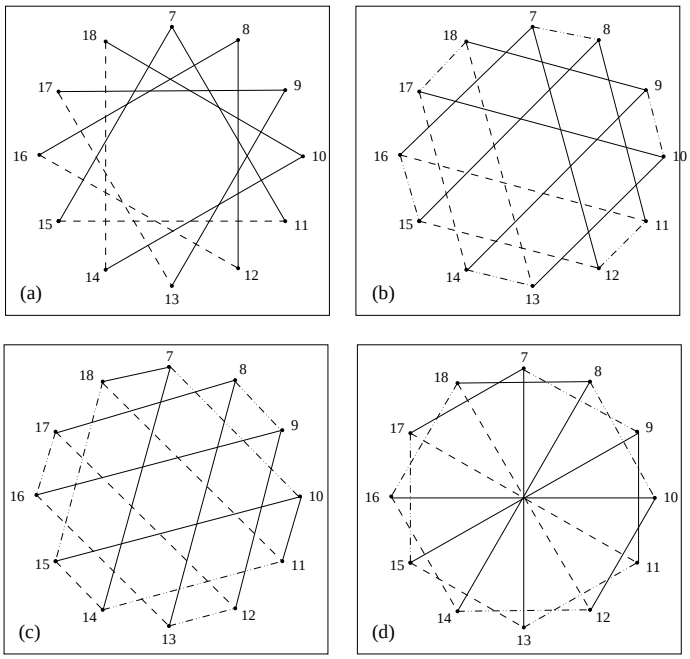

FIG. 8. Diagrammatic representation of groups of transverse observables determining the interference terms of t-matrix elements for the helicity and the transformed helicity basis. The nomenclature for the groups and the corresponding observables are listed in Table XVI for the helicity basis and in Table XVII for the transformed helicity basis.

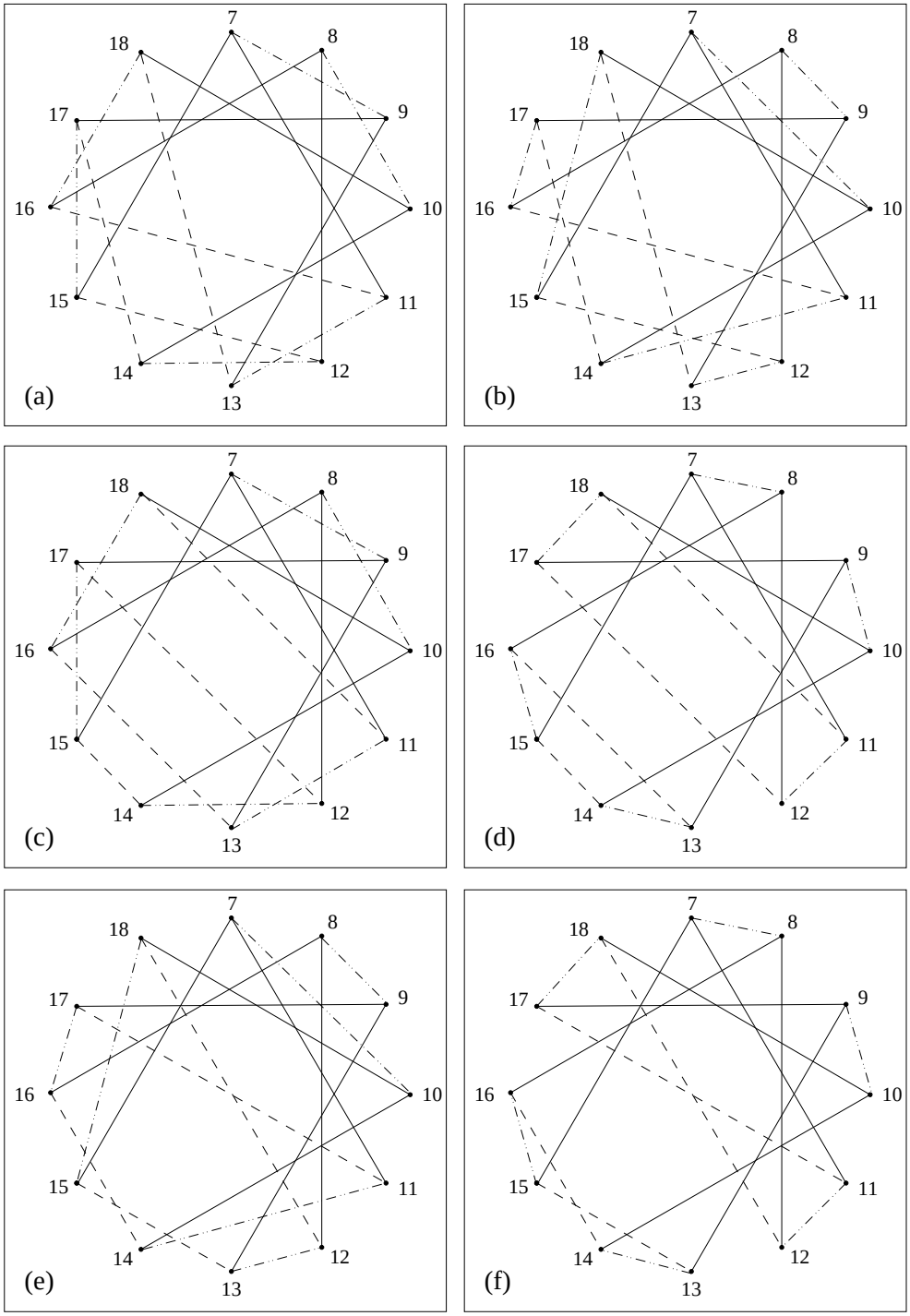

FIG. 9. Diagrammatic representation of three groups of transverse observables leading to a connected diagram for all interference terms allowing a complete determination of eleven t-matrix elements as function of the remaining one for the helicity or the transformed helicity basis. The corresponding observables are explained in the text.